



# NBS TECHNICAL NOTE 1128

U.S. DEPARTMENT OF COMMERCE / National Bureau of Standards

## An Oxygen Consumption Technique for Determining the Contribution of Interior Wall Finishes to Room Fires

0  
0  
5753  
0.1128  
930

## NATIONAL BUREAU OF STANDARDS

The National Bureau of Standards<sup>1</sup> was established by an act of Congress on March 3, 1901. The Bureau's overall goal is to strengthen and advance the Nation's science and technology and facilitate their effective application for public benefit. To this end, the Bureau conducts research and provides: (1) a basis for the Nation's physical measurement system, (2) scientific and technological services for industry and government, (3) a technical basis for equity in trade, and (4) technical services to promote public safety. The Bureau's technical work is performed by the National Measurement Laboratory, the National Engineering Laboratory, and the Institute for Computer Sciences and Technology.

**THE NATIONAL MEASUREMENT LABORATORY** provides the national system of physical and chemical and materials measurement; coordinates the system with measurement systems of other nations and furnishes essential services leading to accurate and uniform physical and chemical measurement throughout the Nation's scientific community, industry, and commerce; conducts materials research leading to improved methods of measurement, standards, and data on the properties of materials needed by industry, commerce, educational institutions, and Government; provides advisory and research services to other Government agencies; develops, produces, and distributes Standard Reference Materials; and provides calibration services. The Laboratory consists of the following centers:

Absolute Physical Quantities<sup>2</sup> — Radiation Research — Thermodynamics and Molecular Science — Analytical Chemistry — Materials Science.

**THE NATIONAL ENGINEERING LABORATORY** provides technology and technical services to the public and private sectors to address national needs and to solve national problems; conducts research in engineering and applied science in support of these efforts; builds and maintains competence in the necessary disciplines required to carry out this research and technical service; develops engineering data and measurement capabilities; provides engineering measurement traceability services; develops test methods and proposes engineering standards and code changes; develops and proposes new engineering practices; and develops and improves mechanisms to transfer results of its research to the ultimate user. The Laboratory consists of the following centers:

Applied Mathematics — Electronics and Electrical Engineering<sup>2</sup> — Mechanical Engineering and Process Technology<sup>2</sup> — Building Technology — Fire Research — Consumer Product Technology — Field Methods.

**THE INSTITUTE FOR COMPUTER SCIENCES AND TECHNOLOGY** conducts research and provides scientific and technical services to aid Federal agencies in the selection, acquisition, application, and use of computer technology to improve effectiveness and economy in Government operations in accordance with Public Law 89-306 (40 U.S.C. 759), relevant Executive Orders, and other directives; carries out this mission by managing the Federal Information Processing Standards Program, developing Federal ADP standards guidelines, and managing Federal participation in ADP voluntary standardization activities; provides scientific and technological advisory services and assistance to Federal agencies; and provides the technical foundation for computer-related policies of the Federal Government. The Institute consists of the following centers:

Programming Science and Technology — Computer Systems Engineering.

<sup>1</sup>Headquarters and Laboratories at Gaithersburg, MD, unless otherwise noted; mailing address Washington, DC 20234.

<sup>2</sup>Some divisions within the center are located at Boulder, CO 80303.

# An Oxygen Consumption Technique for Determining the Contribution of Interior Wall Finishes to Room Fires

NATIONAL BUREAU  
OF STANDARDS  
LIBRARY  
JUL 25 1980

Not acc. - Circ  
QC100  
• US753  
no. 1128  
1980  
C.2

Darryl L. Sensenig

Center for Fire Research  
National Engineering Laboratory  
National Bureau of Standards  
Washington, D.C. 20234

Sponsored in part by:

Armstrong Cork Company  
Lancaster, Pennsylvania 17604



*t* Technical note

U.S. DEPARTMENT OF COMMERCE, Philip M. Klutznick, Secretary

Luther H. Hodges, Jr., Deputy Secretary

Jordan J. Baruch, Assistant Secretary for Productivity, Technology and Innovation

S. NATIONAL BUREAU OF STANDARDS, Ernest Ambler, Director

Issued July 1980

National Bureau of Standards Technical Note 1128

Nat. Bur. Stand. (U.S.), Tech. Note 1128, 87 pages (July 1980)

CODEN: NBTNAE

U.S. GOVERNMENT PRINTING OFFICE

WASHINGTON: 1980

---

For sale by the Superintendent of Documents, U.S. Government Printing Office, Washington, D.C. 20402  
Price \$3.75

(Add 25 percent for other than U.S. mailing)

## TABLE OF CONTENTS

	<b>Page</b>
LIST OF FIGURES . . . . .	v
LIST OF TABLES . . . . .	vi
NOMENCLATURE . . . . .	vii
ABBREVIATIONS . . . . .	ix
Abstract . . . . .	1
1. INTRODUCTION . . . . .	2
2. DETERMINATION OF HEAT RELEASE BY OXYGEN CONSUMPTION . . . . .	5
2.1 Rate of Heat Release . . . . .	5
2.2 Effective Heat of Combustion . . . . .	8
3. APPLICATION OF OXYGEN CONSUMPTION TECHNIQUE . . . . .	9
3.1 Laboratory Bench Test for Determining Rate of Heat Release and Effective Heat of Combustion . . . . .	9
3.1.1 Construction Details . . . . .	9
3.1.2 Verification of Method . . . . .	11
3.1.3 Illustration of Typical Results . . . . .	12
3.2 Quarter-Scale Model Compartment . . . . .	14
3.2.1 Construction Details . . . . .	14
3.2.2 Apparatus to Measure Rate of Heat Release from Burning Materials in Model Compartment . . . . .	17
3.2.3 Convected Heat Through Doorway and Verification of Method . . . . .	19
3.2.4 Method of Obtaining Rate of Heat Release Per Unit Area of Burning Surface in Model Compartment . . . . .	20
3.3 Full-Scale Room Burns -- Details of Room and Exhaust Collection System . . . . .	21
4. RESULTS . . . . .	22
4.1 Quarter-Scale Model Compartment . . . . .	22
4.1.1 Total Heat, Convected Heat, Upper Room Air Temperature, Wall Ignition Time, and Flashover . . . . .	22
4.1.2 Area and Rate of Heat Release Per Unit Area of Burning Wall at Various Times Prior to Flashover . . . . .	25
4.2 Full-Scale Room Burn . . . . .	26
4.3 Laboratory Bench Tests . . . . .	29
4.3.1 Rate of Heat Release . . . . .	29
4.3.2 Flame Spread . . . . .	31
4.4 Comparison of Heat of Combustion With Effective Heat of Combustion . . . . .	33
5. RATIONALIZATION OF OBSERVED FLASHOVER TIMES IN MODEL COMPARTMENT . . . . .	34
6. SUMMARY . . . . .	36
7. RECOMMENDATIONS . . . . .	38
8. ACKNOWLEDGMENTS . . . . .	39
9. REFERENCES . . . . .	40

TABLE OF CONTENTS (continued)

	Page
APPENDIX A. Technical Data . . . . .	A-1
APPENDIX B. Scanning Technique Used to Determine Mean Velocity Across the Exhaust Pipe Cross Section . . . . .	B-1
APPENDIX C. Crib Tests . . . . .	C-1
APPENDIX D. Errors in Calculation of the Rate of Heat Release . . . . .	D-1

## LIST OF FIGURES

Page

Figure 1.	Apparatus for measuring rate of heat release by oxygen consumption . . . . .	41
Figure 2.	Comparison of the rate of heat release from burning methane of known heat of combustion (HOC) at various flow rates with rate of heat release by oxygen consumption . . . . .	42
Figure 3.	Comparison of the rate of heat release from burning methane at a flow rate of 2.53 l/min (1.43 kW) with rate of heat release by oxygen consumption . . . . .	43
Figure 4.	Rate of heat release -- Ohio state calorimeter and oxygen consumption bench test comparison . . . . .	44
Figure 5.	Rate of heat release and effective heat of combustion of 16-mm particleboard (~50% RH) -- bench test results . . . . .	45
Figure 6.	Rate of heat release and effective heat of combustion of 16-mm particleboard at 0% and 50% RH -- bench test results . . . . .	46
Figure 7.	Model compartment -- sketch . . . . .	47
Figure 8.	Model compartment -- cross section . . . . .	48
Figure 9.	Quarter-scale model compartment . . . . .	49
Figure 10.	Full size room . . . . .	49
Figure 11.	Comparison of convected heat into hood with total rate of heat release measured by oxygen consumption from burning methane at various rates of heat release . . . . .	50
Figure 12.	Model compartment results -- 12-mm low density wood fiberboard . . . . .	51
Figure 13.	Model compartment results -- 16-mm particleboard . . . . .	52
Figure 14.	Model compartment results -- 2-ply 6-mm hardboard . . . . .	53
Figure 15.	Area of burning wall involved at various times to flashover, quarter-scale model compartment -- 12-mm low density wood fiberboard . . . . .	54
Figure 16.	Area of burning wall involved at various times to flashover, quarter-scale model compartment -- 16-mm particleboard . . . . .	55
Figure 17.	Area of burning wall involved at various times to flashover, quarter-scale model compartment -- 2-ply 6-mm hardboard . . . . .	56
Figure 18.	Area of burning wall involved at various times, full-scale room burn -- 12-mm low density wood fiberboard . . . . .	57
Figure 19.	Area of burning wall involved at various times to flashover, full-scale room burn -- 2-ply 6-mm hardboard . . . . .	58
Figure 20.	Upper room-air temperature in center of room for full- and quarter-scale enclosures lined with hardboard at 0% RH as a function of rate of heat release as determined by oxygen consumption . . . . .	59

LIST OF FIGURES (continued)

	Page
Figure 21. Rate of heat release -- low density wood fiberboard bench test results . . . . .	60
Figure 22. Rate of heat release -- particleboard bench test results . . . . .	61
Figure 23. Rate of heat release -- hardboard bench test results . . .	62
Figure 24. Flame spread distance vs time -- low density fiberboard . .	63
Figure 25. Flame spread distance vs time -- hardboard . . . . .	64
Figure 26. Rate of flame spread as a function of surface temperature . . . . .	65
Figure 1C. Rate of heat release from 3.4 kg cribs of polyurethane and sugar pine under large hood . . . . .	C-2

LIST OF TABLES

	Page
Table 1. Heat produced per volume of oxygen consumed for some common materials . . . . .	66
Table 2. Comparison of effective net heats of combustion with actual gross and net heat of combustion (MJ/kg) . . . . .	67
Table 3. Data summary for prediction of flashover times in model compartment . . . . .	67

## NOMENCLATURE

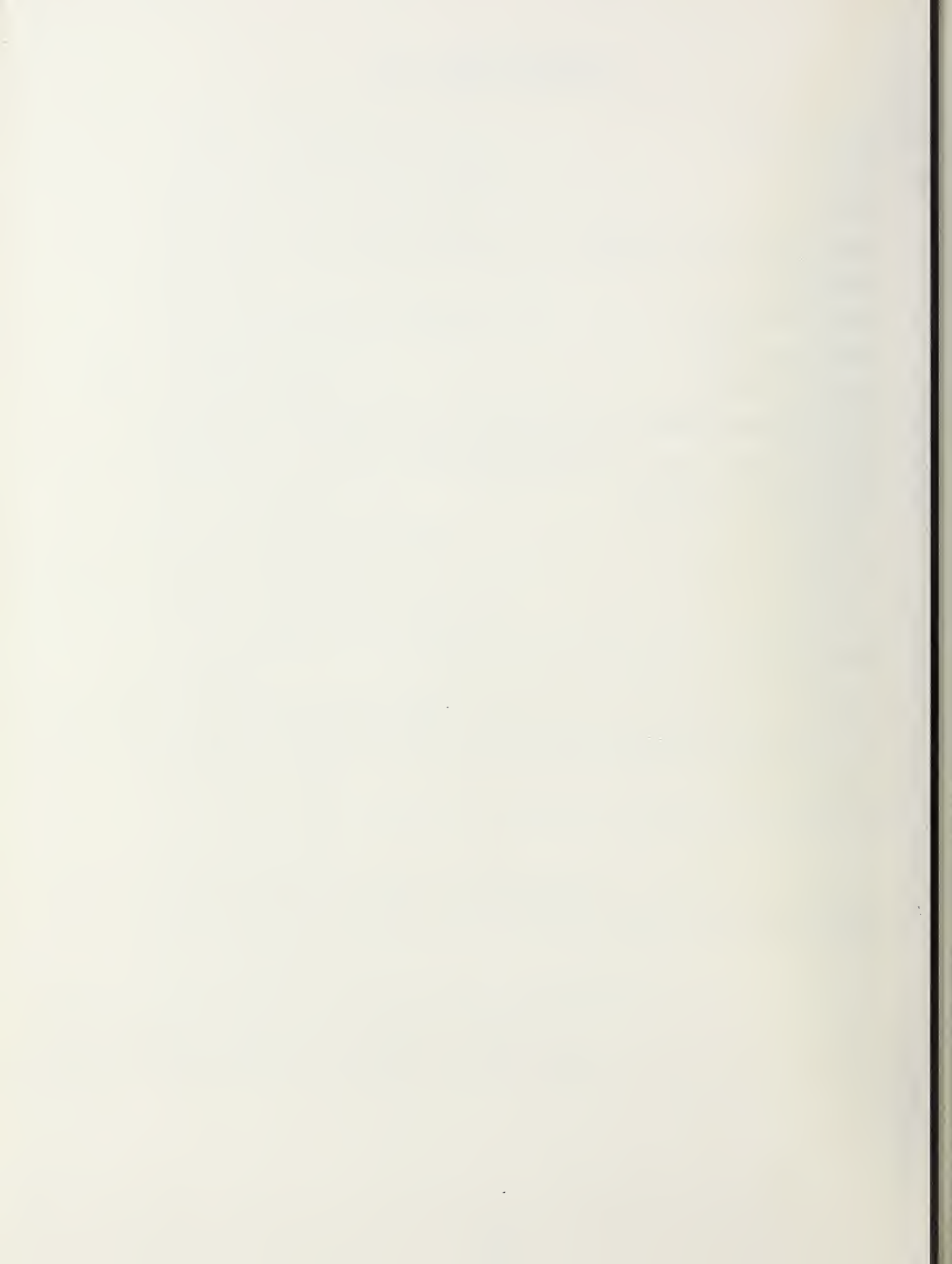
A	= Cross sectional area of exhaust duct (m <sup>2</sup> )
a	= Number of carbon atoms in fuel molecule
b <sup>2</sup>	= Number of hydrogen atoms in one fuel molecule
c	= Number of oxygen atoms in one fuel molecule
C	= Heat capacity (kJ/kg K)
C <sub>4</sub>	= Empirical constant defined by equation 13
C <sub>v</sub>	= Ratio of average velocity to centerline velocity in the exhaust duct
ΔP	= Pitot-static tube differential pressure (Pa)
ΔT	= T <sub>1</sub> - T <sub>A</sub> (K)
D	= Density of saturated water vapor in air (g/m <sup>3</sup> )
E	= Oxygen analyzer output during test (volts)
E <sub>0</sub>	= Oxygen analyzer output with normal air (volts)
F	= Characteristic flame spread constant (m K <sup>2</sup> /s)
h	= Height of door (m)
H	= Heat flux to surface (kW/m <sup>2</sup> )
λ	= Thermal conductivity (kW/m K)
λ	= Length of preheating region for flame spread (m)
L	= Length of boundary between burning and non-burning area (m)
ṁ	= Mass flow rate (kg/s)
ṁ <sub>a</sub>	= Molar flow rate of air into system
ṁ <sub>A</sub>	= Molar flow rate of argon into system
ṁ <sub>H<sub>2</sub>O</sub>	= Molar flow rate of water vapor into system
ṁ <sub>N<sub>2</sub></sub>	= Molar flow rate of nitrogen into system
ṁ <sub>O<sub>2</sub></sub>	= Molar flow rate of oxygen into system
ṁ <sub>s</sub>	= Molar flow rate of combustion gases in the exhaust duct
Q	= Total rate of heat release (kW)
Q <sub>c</sub>	= Rate of convected heat through the doorway (kW)
q̄	= Mean rate of heat release per unit area (kW/m <sup>2</sup> )
Q*	= Critical rate of heat release at flashover in model compartment (kW)
R	= Relative humidity (%)
ρ	= Density (kg/m <sup>3</sup> )

## NOMENCLATURE (continued)

$\rho_o$	= Density of ambient air ( $\text{kg}/\text{m}^3$ )
$\rho_o^*$	= Density of ambient air (g/mole)
$\rho_s$	= Density of stack gases ( $\text{kg}/\text{m}^3$ )
$\rho_s^*$	= Density of stack gases (g/mole)
$t$	= Time (s)
$t^*$	= Time from ignition to flashover (s)
$t_{fo}$	= Flashover time (s)
$t_{ig}$	= Ignition time (s)
$T$	= Temperature of exhaust gas at point of pressure measurement (K)
$T_1$	= Temperature of exhaust gas entering hood (K)
$T_a$	= Ambient temperature (K)
$T_o$	= Standard temperature (298 K)
$T_p$	= Pyrolysis temperature (K)
$T_s$	= Material surface temperature (K)
$\theta$	= Oxygen depletion - the fraction of incoming oxygen molecules removed by combustion
$v_F$	= Flame spread velocity (m/s)
$\dot{V}_a$	= Volume flow rate of air into the system referred to standard conditions ( $\text{m}^3/\text{s}$ )
$\dot{V}_s$	= Volume flow rate of exhaust gas referred to standard conditions ( $\text{m}^3/\text{s}$ )
$w$	= Width of door (m)
$x_c$	= Volume fraction of oxygen in the analyzer
$x_c^o$	= Volume fraction of oxygen in the analyzer prior to the test (oxygen concentration of dry air)
$x_H$	= Volume fraction of water vapor in normal air
$x_o$	= Volume fraction of oxygen in normal air
$x_s$	= Volume fraction of oxygen in exhaust duct

## ABBREVIATIONS

CH - Convected heat  
FB - Fiberboard  
FO - Flashover  
FSC - Flame spread classification  
HB - Hardboard  
HOC - Heat of combustion  
MC - Model compartment  
RH - Relative humidity  
RHR - Rate of heat release  
RWL - Rate of weight loss  
URT - Upper room temperature



AN OXYGEN CONSUMPTION TECHNIQUE FOR DETERMINING THE  
CONTRIBUTION OF INTERIOR WALL FINISHES TO ROOM FIRES

Darryl L. Sensenig<sup>1</sup>

An oxygen consumption technique was developed for determining the total rate of heat production in a room fire. This was accomplished by measuring the volume flow rate and the oxygen concentration of the exhaust gases flowing through a collection hood. This method can be used with unknown combinations of burning materials including both interior finish and furnishings. By simultaneously measuring the rate of oxygen consumption and the rate of mass loss the effective heat of combustion of the wall linings were determined in a reduced-scale model room fire test. The average heat release rate per unit area of the wall linings was determined by recording the area of involvement during the test and dividing this area into the total rate of heat production at that time. The enthalpy of the exhaust gases passing out of the doorway was determined with the aid of an array of thermocouples located at the entrance to the exhaust duct. By subtracting the enthalpy flow through the doorway from the total rate of heat production in the room, the heat losses through the bounding surfaces were determined. Reduced-scale and full-scale room fire tests and a bench test for heat release rate using the oxygen consumption technique

<sup>1</sup>This work was conducted from September 1976 to September 1977 while Mr. Sensenig was a research associate at the National Bureau of Standards for the Armstrong Cork Company.

are discussed in this report. Lateral flame spread rates on vertical surfaces measured in the model room fire tests and in a laboratory bench test are also described.

Key words: Fire tests; flame spread; flashover; heat release rate; ignition; interior finish; oxygen depletion; room fires.

## 1. INTRODUCTION

The flame spread classification (FSC) obtained by the ASTM E-84 tunnel test [1]<sup>2</sup> is generally used by the building codes to regulate the surface burning characteristics of interior finish materials. However, in order to predict the actual contribution of these materials to fire growth in a room it is necessary to perform expensive large-scale room fire tests. The number of such tests may be reduced if a reliable analytical prediction model can be developed which uses the fire properties of the interior finish materials as input data. A complete analytical description of the fire development in a room is extremely complex, considering the interactions of combustion chemistry, heat transfer and fluid mechanics. Even the simplest fire remains to be satisfactorily described. Much of the difficulty in the development of a valid analytical model stems from the inability to properly interpret and use fire descriptors such as the ignitability, rate of heat release (RHR), and rate of flame spread on materials as obtained from laboratory fire tests. The influence of each of these "fire properties," as expressed by numerical values from standardized laboratory tests, on room fire buildup has been assessed by Fang [2].

---

<sup>2</sup>Numbers in brackets refer to the literature references listed at the end of this report.

A major effort is currently being devoted to the development of the mathematical models. This requires reliable comparisons of the fire properties of interior finish materials as they exist in room fires with those measured in laboratory tests under conditions approximating those in the room. It also requires reliable comparisons with important parameters in room fire tests such as the total rate of heat production and the total heat loss rate through the bounding surfaces of the room. There are no methods currently available to determine these important quantities when combustible interior finish is involved in the fire. There are heat release rate calorimeters [3,4] which can be used to measure the heat release rate per unit area as a function of the external radiant flux. However, in order to establish the proper exposure conditions in these calorimeters it is necessary to compare these measured heat release rates with the heat release rate per unit area of the burning material measured in a room fire. There has been no way of obtaining the latter quantity.

A method based on oxygen consumption was investigated as a means of measuring the instantaneous rate of heat production in the room fire. This technique is based on the observation that for a given volume of oxygen consumed there is a fixed amount of heat released, nearly independent of the type of material burned [5].

As combustible volatiles are being released during the fire, air containing oxygen for their combustion enters the room through the lower part of the doorway. The oxygen depleted gases are exhausted through the upper part of the doorway serving as the single exit. Combustion can occur totally within the compartment or flames can extend through the doorway as a result of excessive volatilization. In either case, by analyzing the combustion products collected in an exhaust system positioned above the doorway, the amount of oxygen consumed in the burning process can be measured. Multiplying the volume rate of oxygen consumed by the heat produced per unit volume of oxygen provides a direct measure of the rate of heat released from the burning materials within the compartment. 3

In order to verify the oxygen consumption technique for measuring heat produced, it was first studied as a laboratory bench test, and then applied to a quarter-scale model compartment fire and finally to a full size room fire. The rate of heat release was measured by this method on small vertical specimens in the bench test for various conditions of ignition, heat flux and preheat. These conditions had a significant influence on the curves for the rate of heat release per unit area versus time. In order to determine the most suitable conditions for direct application to the room fire, model compartment fire tests were conducted. A quarter-scale model of a 3 x 3 x 2.4 compartment containing combustible walls, a noncombustible ceiling and no furnishings was constructed for this purpose. The fire buildup created in the model compartment by the combustible interior wall finishes was assessed visually and by measurements of the total rate of heat release, area of involvement, temperatures and heat fluxes. Accurate determination of the total rate of heat release and the instantaneous burning area of the compartment walls permitted comparisons with laboratory test measurements of the rate of heat release per unit area. These comparisons then suggested the most appropriate exposure conditions in the laboratory test for direct application of these data to predict the fire buildup in the model compartment. The rate of heat produced obviously depends on the area burning, therefore, another study was conducted in order to obtain basic information on rate of flame spread. Many standardized "flame spread" tests exist; e.g., ASTM E 84, ASTM E 162, etc., but for proper comparison, it is necessary to select conditions of exposure and methods of computation that describe quantitatively the flame spread along the wall surfaces within the room. In an attempt to simulate the lateral flame spread occurring on the walls in the model room, a bench test was set up to determine the rate of horizontal flame spread on a vertical surface as a function of surface temperature.

The time to ignition of the wall is another important parameter that must be considered in developing an analytical model describing fire buildup in a room. This parameter was investigated with a gas diffusion burner,

representing a small quantity of burning contents or a small ignition source placed in the corner of the compartment with the flames impinging on the wall.

This study provides important information on the proper interpretation and use of laboratory test data for their eventual application to an analytical approach for predicting fire buildup in a room, up to and including flashover. Flashover is defined here as the condition when there is sufficient radiation from the heated gases and upper room surfaces to ignite light combustible materials in the lower part of the room.

## 2. DETERMINATION OF HEAT RELEASE BY OXYGEN CONSUMPTION

### 2.1 Rate of Heat Release

A method for measuring the heat release rate of burning materials was described by Parker [5] in connection with the ASTM E 84 tunnel test. This method is based on the assumption that for a given volume of oxygen consumed there is a fixed amount of heat released, nearly independent of the type of material burned even though the heats of combustion may be considerably different as seen in table 1. Similar computations were made from a table of heats of combustion of organic compounds listed in the Handbook of Chemistry and Physics [8]. The heat produced per volume of oxygen consumed was found to be  $16.7 \text{ MJ/m}^3$  with a range of  $\pm 1 \text{ MJ/m}^3$  at  $25^\circ\text{C}$  and one atmosphere pressure.<sup>3</sup> The product of this constant and the volume rate of oxygen consumption provides a direct measure of the rate of heat release from a burning object. A small correction needs to be applied for carbon monoxide

---

<sup>3</sup>A more comprehensive review of the heat release per volume of oxygen consumed done after the completion of this work suggests that a better value would be  $17.1 \text{ MJ/m}^3$ , i.e., an increase of 3% [6]. This difference arises partly because the calculations on which table 1 were based assumed that all the hydrogen went to water, whereas, for example, in PVC part of the hydrogen goes to HCl; also the value for cellulose in table 1 was based on a value of  $16.7 \text{ MJ/kg}$  for the gross heat of combustion whereas a better value is  $17.5 \text{ MJ/kg}$  [7].

when it is formed in significant quantities since the heat release per volume of oxygen consumed for combustion to CO ( $10.3 \text{ MJ/m}^3$ ) is significantly less than for combustion to  $\text{CO}_2$ . Measurement of the  $\text{CO}/\text{O}_2$  ratio in the combustion products should permit a suitable correction; however, it was not accounted for in this study. The heat release rates discussed in this report are based on the net heat of combustion (i.e., the water formed is assumed to be in the gaseous state).

The volume rate of oxygen consumption was measured by collecting all of the combustion products from a burning object along with an arbitrary amount of surrounding makeup air. This mixture of air and combustion gases was collected in a hood and discharged at a measured volume flow rate and temperature through an exhaust duct where it was analyzed for oxygen concentration. When there is no burning taking place, 20.8 percent of the volume discharged is oxygen, assuming 293 K and 40% RH. For dry air the normal oxygen concentration is 21 percent [5]. However, when burning occurs, the percentage of oxygen in the flow discharged is lowered. The rate of heat production,  $\dot{Q}$ , is proportional to the rate of oxygen consumption which is equal to the difference between the oxygen flowing into and out of the system

$$\dot{Q} = 1.67 \times 10^4 (x_o \dot{v}_a - x_s \dot{v}_s) \quad (1)$$

where  $x_o$  is volume fraction of oxygen in normal air,  $\dot{v}_a$  is the volume flow rate of air into the system,  $x_s$  is the volume fraction of oxygen in the exhaust duct and  $\dot{v}_s$  is the total volume flow rate in the duct where  $\dot{v}_a$  and  $\dot{v}_s$  refer to standard conditions. Note that  $\dot{Q}$  in equation 1 is expressed in kW while the heat produced per volume of oxygen consumed is in  $\text{MJ/m}^3$  thus the factors of  $10^3$  in the numerical coefficient. It was assumed that  $\dot{v}_a = \dot{v}_s$  and that the oxygen concentration in the oxygen analyzer was the same as that in the exhaust duct. Then

$$\dot{Q} = 1.67 \times 10^4 \dot{v}_s x_o \left( \frac{x_o - x_s}{x_o} \right) = 1.67 \times 10^4 \dot{v}_s x_o \theta \quad (2)$$

where the oxygen depletion,  $\theta$ , is defined within the limitations of these assumptions as  $\theta \equiv \frac{X_O - X_S}{X_O}$ . While these assumptions are not strictly correct, the approximation is adequate for organic solids at small oxygen depletions. The extent of the error introduced is examined in appendix D. From equation 2 it is seen that the effect of adding dilution air is simply to increase  $V_S$  and decrease  $\theta$  while keeping their product constant for the same heat release rate.

The volume flow rate in the stack referred to standard conditions is given by

$$\dot{V}_S = C_V A \left( \frac{2}{\rho_O} \frac{P_O}{P} \frac{T_O}{T} \right)^{1/2} (\Delta P)^{1/2} \quad (3)$$

where  $C_V$  is the ratio of the average velocity in the stack to the centerline velocity (0.85 for the 5.08 cm diameter stack used in these experiments).

$A$  is the cross sectional area of the stack ( $2.03 \times 10^{-3} \text{ m}^2$ )

$\rho_O$  is the density of ambient air ( $1.18 \text{ kg/m}^3$ ),

$P_O$  is the standard pressure ( $1.01 \times 10^5 \text{ Pa}$ , 760 mm Hg),

$P$  is the ambient pressure (Pa),

$T_O$  is the standard temperature (298 K),

$T$  is the temperature in the stack (K),

$\Delta P$  is the pressure difference across the pitot-static tube (Pa).

It was assumed that the ambient density of the stack gases is the same as air. The error introduced is small and is discussed in appendix D. Then

$$\dot{Q} = 1.67 \times 10^4 X_O C_V A \left( \frac{2}{\rho_O} \frac{P_O}{P} \frac{T_O}{T} \right)^{1/2} (\Delta P)^{1/2} \theta \quad (4)$$

or substituting in the values for the above quantities assuming  $\frac{P_O}{P} = 1$

$$\dot{Q} = 134 (\Delta P/T)^{1/2} \theta \quad (5)$$

Experimentally,

$$\theta = \frac{E_O - E}{E_O} \quad (6)$$

where  $E_0$  and  $E$  are the oxygen analyzer output voltages for ambient and test conditions respectively. It is assumed that the analyzer has a linear output and that  $E = 0$  when  $X_{O_2} = 0$ . It was assumed in equation 5 that  $X_0 = 0.208$  which is the oxygen volume fraction of normal air at 293 K and 40% RH. The calculation of the rate of heat release by this technique neglects the increase in molar flow rate in the duct due to the generation of gases in the fire which pass through the system uncombusted or produce more moles of combustion products than the moles of oxygen consumed.

## 2.2 Effective Heat of Combustion

The heat of combustion is generally obtained by burning a specimen of known weight in a pure oxygen atmosphere within a pressurized "bomb" and measuring the total heat liberated. A material undergoes complete oxidation under these conditions, which is often uncharacteristic of that which occurs in a room fire. The potential heat of a material, defined as the difference between its heat of combustion and the product of the mass fraction and the heat of combustion of the residue remaining after exposure to a simulated standard fire (750°C for 2 hours), is a method of taking into account a more realistic fire condition [9]. Most organic materials undergo complete combustion to  $CO_2$  and  $H_2O$  in the potential heat test. However, in the room fire, flaming combustion of many materials is accompanied by a char forming process which reduces the effective heat of combustion during the flaming phase. The char structure formed has a much higher heat of combustion, which is released during the glowing combustion stage of the fire. In order to obtain the effective heat of combustion of materials under conditions simulating the early stages of a room fire, a load cell was built into the bench test for the rate of heat release so that the rate of weight loss and rate of heat release could be obtained simultaneously.

The rate of mass loss was computed from the difference in mass between 15 seconds prior to and 15 seconds after the time of the oxygen determination.

The ratio of the rate of heat release to the rate of mass loss is the instantaneous effective heat of combustion which was measured as a function of time throughout the test. If the specimen is completely consumed except for its ash, the integral of the heat release rate over the duration of the test divided by the total mass loss should yield the net heat of combustion. This can be compared with the gross heat of combustion obtained in the oxygen bomb calorimeter if the specimen is completely consumed and a suitable correction has been made for the heat of condensation of the water formed during the combustion.

### 3. APPLICATION OF OXYGEN CONSUMPTION TECHNIQUE

#### 3.1 Laboratory Bench Test for Determining Rate of Heat Release and Effective Heat of Combustion

##### 3.1.1 Construction Details

A schematic of the apparatus is shown in figure 1. The specimen was placed in a holder designed so that burning was restricted to the front surface, which was exposed to the flame and/or radiant flux, and could not occur along the specimen edges. The specimen was placed on a 0.5 kg capacity water cooled strain gauge load cell calibrated for a sensitivity of 50 g/V and was positioned directly beneath a hood to collect the combustion products. The combustion gases, as well as the surrounding makeup air, were drawn into the hood and through a pipe of 50.8 mm diameter and 1.5 m length by a squirrel cage blower operating at a nominal flow rate of  $0.7 \text{ m}^3/\text{min}$ . A pitot-static tube and a thermocouple were placed in the center of the flow stream at the mid length of the pipe to measure the velocity and temperature needed for the volume flow calculations. The mean velocity across the pipe cross section was found to be 0.85 of the maximum velocity in the center of the pipe. This correction is due to the shape velocity profile which was

determined by scanning the cross section of the pipe with a pitot-static tube using the averaging scheme found in the literature supplied by the manufacturer of the pitot tubes (see appendix B).

The oxygen concentration in the exhaust stream was measured with an electrochemical oxygen cell which uses a KCl solution with gold and zinc electrodes. A tube for sampling the gas was placed in the exhaust pipe down stream from the pitot-static tube and the thermocouple. The sample of exhaust gas first passed through a dry ice cold trap and a glass fiber filter to remove water and particulates and then through a vacuum pump. A valve in line with a rotameter between the oxygen cell and the exhaust from the vacuum pump was set to produce a flow rate of  $16 \text{ cm}^3/\text{s}$  through the cell. The cell has an output voltage proportional to the oxygen concentration. A  $300 \text{ k}\Omega$  10 turn potentiometer placed across the output of the cell provided a means of adjusting the output voltage to 100 mV when normal room air was being measured. An output reading of 0 mV was set to correspond to 0 percent oxygen using pure nitrogen. Millivolt deviations from 100 mV then are read directly as percent oxygen depletions which are used in the calculation of rate of heat release.

Since the heat losses do not affect the calculated rate of heat release, adiabatic chambers or constant temperatures within a confined space are not necessary. In fact, the specimen is in an open environment without visual restrictions except for the electric panel radiant heat source placed in front of it for exposure to various heat flux levels. A study of the effect of reduced oxygen levels on the rate of heat release would require enclosing the specimen in a chamber. This was considered beyond the scope of the study, but could be significant in cases where materials are burning in reduced oxygen atmospheres. Ignition of the specimen was accomplished with a gas pilot burner. A small pilot burner placed near the top or bottom of the specimen may not make an appreciable contribution to the rate of heat release. However, if the pilot is a line burner as shown in figure 1 and the gas flow

rate is large enough to actually bathe the specimen in flame a correction must be made for the heat produced by the burner.

### 3.1.2 Verification of Method

The oxygen consumption method for determining the rate of heat release was verified by burning a material of known heat output beneath the collection hood. Methane (technical grade) was used since its heat of combustion and flow rate were accurately known. It was burned at various flow rates and the results of the comparison of this known RHR with the measured RHR by  $O_2$  consumption is shown in figure 2. This shows that the RHR results are directly proportional under steady-state conditions with an accuracy of  $\pm 10\%$ .

Shown in figure 3 are the results of a step increase in gas flow. The broken line in figure 3 is the computed rate of heat release from the burning of the methane gas at a volume flow rate of 2.53 l/min with a net heat of combustion of  $34 \text{ MJ/m}^3$  corresponding to 1.43 kW. The solid line is the computed rate of heat release as a function of time determined by the oxygen consumption method. Good agreement was obtained with the exception of a short period following ignition and extinguishment where the steady-state value was reached relatively slowly due to the limited time response of the measurement system for the oxygen concentration. This time response, which was about 20 seconds for a step increase to reach 95 percent of its final value, may be a source of dynamic error for cases where rapid changes occur, but in most cases, e.g., for the solid materials examined in this report, this time response is sufficiently fast. For materials exhibiting more rapid changes in the rate of heat release, a computer correction can be utilized similar to the numerical technique used to correct the Ohio State University (OSU) heat release rate calorimeter data for apparatus delay [10].

Another means of verification of the oxygen consumption method is to compare results with those obtained by other calorimetric techniques. The rates of heat release of four materials were measured using the Ohio State University calorimeter [4] and the oxygen consumption method. The OSU data was corrected for time response according to reference 10. The results are compared in figure 4. The specimen holder, specimen size 15.2 x 15.2 cm, mounting technique, pilot ignition, and heat flux were identical for both test methods in order to eliminate some of the possible sources of variation. The results shown represent single runs on each apparatus rather than averages, since only one test was conducted on each material by each method.

The agreement is quite good, perhaps better than would be expected, since the differences are not much more than might be obtained from repeatability checks on the same equipment. Slight discrepancies did exist prior to the test termination for the fiberboard and polyurethane, but this was due to specimen fallout and combustion occurring on the back of the specimen earlier in one test than in the other.

### 3.1.3 Illustration of Typical Results

Several rate of heat release test results on 16-mm thick particleboard are shown in figures 5 and 6. These plots demonstrate typical results that were obtained for an easily ignitable material with this equipment. In figure 5 the three curves for the rate of heat release were obtained at incident radiant exposures of 2, 2.5, and 3 W/cm<sup>2</sup>. The exposure of the specimen begins at time 0. There is a time delay before ignition and heat release occurs; this depends upon the time required to attain the pyrolysis temperature. During this time, the surface temperature increases until the pilot flame at the bottom ignites the gases released from a small portion of the specimen exposed to the pilot flame. The surface temperature of the specimen continues to increase and the flame traverses the specimen surface until the entire surface is aflame. Prior to total surface involvement, the

computed rate of heat release per unit area is disproportionately low, since the results are obtained by dividing the rate of heat release by the exposed surface area, even though it is not totally involved. Total surface involvement occurs just prior to the peak heat release rate. The results indicate that the higher the incident heat flux, the higher the peak rate of heat release.

The effective heat of combustion obtained from the ratio of the rate of heat release and the rate of mass loss is also shown in figures 5 and 6. In the initial stages of the test as the temperature reached 100°C, water was vaporized from the surface and the initial rate of mass loss was relatively high compared to the rate of weight loss of the combustible volatiles. Therefore, the effective heat of combustion curve, rather than being a step function, gradually increased until a plateau was reached. The plateau indicates that the effective heat of combustion was essentially constant. Since the plateaus in the curves for the heat of combustion in figure 5 are identical for each exposure condition, it can be concluded that the effective heat of combustion is independent of the radiant exposure over the range tested.

The average effective heat of combustion is approximately 12.5 MJ/kg, which is significantly lower than the net heat of combustion of 17.7 MJ/kg for a specimen of this material conditioned to 50% RH at 23°C as measured in the oxygen bomb calorimeter.

These values are consistent with the fact that the water released in the char forming process dilutes the combustible pyrolysis products and this lowers the effective heat of combustion. Higher values might be expected during the latter stages, but the tests were not carried far enough to obtain a significant contribution from the char which was found to have a heat of combustion of 33 MJ/kg. This argument is supported by figure 1C of

appendix C where an increase in the effective heat of combustion was obtained during the latter stages of combustion of a wood crib.

The effect of the conditioning RH was also examined for its influence on the rate of heat release and effective heat of combustion. The results shown in figure 6 illustrate that predrying of particleboard not only increased the rate of heat release, but also increased the average effective heat of combustion by about 10 percent. The low absorbed water content minimized the endothermic effect of water vaporization and thus permitted a higher rate of temperature rise. This resulted in a higher pyrolysis rate and an increase in the rate of heat release. The effective heat of combustion was increased because the rate of weight loss of the specimens conditioned at 0% RH did not include absorbed water loss.

### 3.2 Quarter-Scale Model Compartment

#### 3.2.1 Construction Details

In order to examine the room fire phenomena in a laboratory size enclosure a quarter-scale model of a 3 x 3 x 2.4 m room with a 0.76 m wide and a 18.4 m high doorway was constructed utilizing the following scaling rules [11,12]:

- (1) Linear dimensions of the room are proportional to the scale factor.
- (2) Height of doorway is proportional to the scale factor.
- (3) Width of doorway is proportional to the square root of the scale factor.
- (4) Thicknesses of the wall and ceiling lining materials are independent of the scale factor.
- (5) Heat release rate of exposure fire is proportional to the square of the scale factor, and
- (6) Times are independent of the scale factor.

Although exact scaling is impossible this procedure has been found to provide a similar fire buildup scenario on the two scales which is adequate to demonstrate the application of the oxygen consumption technique to the study of room fires.

The model compartment constructed for this study (see sketch, figure 7) was designed with two novel features: (1) a simple means of relining the walls with new materials without completely dismantling the instrumentation; (2) the ability to obtain accurate weight losses of the burning walls without errors introduced by attached wires and water lines to transducers and with minimal correction for buoyancy forces on the floor and the ceiling. These features were incorporated for expediency in conducting the tests and to obtain accurate effective heats of combustion of the burning wall linings.

Since the test materials were placed only on the walls, the first design feature was easily accomplished by the use of a removable, noncombustible ceiling. In this way the wall specimens were easily inserted from the top. The specimens were held in position by small clips at the top and bottom of the wall. In order to obtain the weight loss of the walls with minimal corrections from forces on the ceiling and floor, the ceiling and floor were arranged to be completely independent from the walls. A cross section of the model compartment is shown in figure 8. The interior dimensions were  $0.75 \times 0.75 \times 0.60$  m high, and the doorway dimensions were 0.38 m wide by 0.46 m high. There were two independent chambers. The outer chamber was the structural housing forming airtight water seals with the inner chamber, at the floor/wall and ceiling/wall intersections. The compartment ceiling was supported on the walls of the outer chamber, forming an airtight seal preventing leaks of combustion gas, without contacting the inner chamber. The inner chamber, used for holding the combustible walls in position, formed an airtight enclosure except for the doorway and was suspended on three equally spaced load cells located outside of the outer chamber while not contacting the outer chamber. The inner chamber, including the combustible

walls, weighed approximately 75 kg and rested partially on load cells and partially on springs. The load cells and springs were in parallel. The total weight of the inner chamber was initially supported on the springs as shown in detail in figure 8. The adjustment of the load applied to the load cells was accomplished by turning the thumb wheel supporting the spring and inner chamber. This lowered the load cell attached to the support arm until contact was made between the load cell and the pedestal. The thumb wheel was lowered farther until approximately 1 percent of the total 75 kg was supported by each of the three load cells and the remainder supported by the springs. The load cells had spring constants of 18.9 kg/mm, which were much higher than the 0.6 kg/mm for the springs. Therefore, changes in weight of the inner chamber resulted in minimal vertical displacement since most (97%) of the weight change was seen by the load cell. The system was calibrated with a set of weights. This design permitted high resolution of the weight change, which was necessary since less than 1 percent of the total weight of the inner chamber was lost during the burning of the compartment walls up to the time of flashover.

With the requirement that the ceiling not be attached to the inner walls because of buoyancy effects, a small gap was created along the wall/ceiling intersection. The higher pressure in the upper compartment forced the flame to lick back over the top of the inner wall and the flame was no longer confined to traveling along the intersection. Because of this necessity for a tight wall/ceiling intersection, a portion of the ceiling had to be attached to the inner wall as shown in figure 8.

Pressures  $P_1$  and  $P_2$  above and below the ceiling attached to the walls were essentially equal, thus no buoyancy correction was necessary. However, for area  $A_1$  pressures  $P_1$  and  $P_3$  acted downward and upward respectively. Since  $P_3$  was lower than  $P_1$  a downward force was exerted on the inner chamber when the upper room air temperature and pressure increased. A curve of air pressure versus force correction was obtained by conducting burn tests in the

compartment containing noncombustible materials of constant weight. Thus an incremental force correction was applied to all weight loss data used for calculations of the heat of combustion.

Other instrumentation within the compartment consisted of five vertical assemblies "trees" of ten thermocouples each--one tree on each of the three walls for measuring surface temperatures, one in the center of the compartment to measure air temperatures from the floor to the ceiling, and one in the doorway to measure the inflow air and exhaust gas temperatures. No corrections were made for thermocouple radiation error. Radiation to the floor was measured with a heat flux meter placed at floor level in the center of the front left quadrant of the compartment.

A schematic of the model compartment is shown in figure 9. The doorway in the model compartment was positioned off center on the front wall with one side of the doorway 0.02 m from the corner, thus duplicating the physical arrangement used in some previous compartment studies conducted at NBS. A (0.08 x 0.08 m) gas diffusion burner having a flat surface of porous ceramic fiber was used as an igniting source for the wall in the corner diagonally across from the doorway.

The flow rate of the methane to the burner was adjusted to provide a heat input of 2.8 kW for all model compartment tests. This rate of gas flow produced a flame height of approximately one half the wall height.

### 3.2.2 Apparatus to Measure Rate of Heat Release from Burning Materials in Model Compartment

The quarter-scale model compartment was constructed in order to determine the potential contribution of the interior wall finishes to room fires. The oxygen consumption method was employed to determine the rate of heat release. This method was applied to the compartment by placing an

exhaust hood directly above the doorway as shown in the sketch of the apparatus in figure 7 so that the combustion products coming from the room could be collected. The oxygen concentration in the combustion products was measured and the rate of heat release was calculated in the same manner as that used for the laboratory bench test method.

The difference between the exhaust collection system in the bench test and the compartment was basically in the size and in the volume flow rate. The combustion gases exhausted through the doorway of the model compartment, as well as some of the surrounding air, were drawn into the hood by a squirrel cage blower. The mixed gases were forced through a uniform pipe, 0.15 m diameter and 4 m long, at a nominal flow rate of  $7.1 \text{ m}^3/\text{min}$ .

A pitot-static tube and four thermocouples connected in parallel were placed near the center of the flow stream at the mid-length of the exhaust pipe to measure the velocity and the temperature needed for the volume flow calculations.

The mean velocity across the cross section of this pipe as measured by the pitot-static tube was  $C_v = 0.95$  of the maximum velocity measured in the center of the pipe since the shape of the velocity profile was more uniform in this larger diameter pipe. The measurement of the oxygen concentration was identical to that described in section 3.1.1. Also mounted in the exhaust pipe was a light obscuration meter for measuring the smoke generated from the wall linings in the room. Smoke optical density measurements were obtained but are not included in this report as their interpretation is beyond the scope of this project.

### 3.2.3 Convected Heat Through Doorway and Verification of Method

Two important parameters in room fire tests are the total rate of heat production and the total heat loss rate through the bounding surfaces of the room. The total rate of heat production from burning materials within a room can be determined by the oxygen consumption method. This heat is partly absorbed by the interior surfaces of the room and partly radiated and convected through the open doorway. The heat convected through the doorway,  $\dot{Q}_c$ , can be determined by measurements taken in the doorway, but more simply by measurement of the temperature increase and volume flow rate of the gas entering the hood.

$$\dot{Q}_c = \dot{m} C \Delta T \quad (7)$$

where  $\dot{m}$  = mass flow rate,  $C$  = mean heat capacity of air at constant pressure and  $\Delta T$  = temperature difference between the air entering the exhaust hood and the ambient air ( $T_1 - T_a$ ) (assuming that the values of the heat capacity and density of the exhausted combustion products are the same as those of air).

The mass flow rate through the exhaust pipe is equal to the product of  $\dot{V}_s$  and  $\rho$  measured at the pitot-static tube and is the same as that entering the hood. The temperature of the mixture of surrounding makeup air and heated gases from the burning compartment entering the hood was measured with 16 chromel-alumel thermocouples connected in parallel. Eight thermocouples were equally spaced in the duct entrance, 0.08 m above the hood around a circle whose diameter was 0.5 times the diameter of the duct and the remaining eight around a concentric circle whose diameter was 0.8 times that of the duct. Air temperature measurements at the hood entrance are not affected by heat losses in the exhaust system. Thus the enthalpy of the air entering the hood closely approximates the heat convected through the doorway provided there is no burning outside the doorway.

Equation (7) can be written in terms of measured quantities

$$\dot{Q}_c = C_V A C (2 \rho_o T_o)^{1/2} \left( \frac{\Delta P}{T} \right)^{1/2} \Delta T \quad (8)$$

or substituting in the values for  $C_V = 0.95$ ,  $A = 0.0182 \text{ m}^2$ ,  $\rho_o = 1.18 \text{ kg/m}^3$ ,  $T_o = 298 \text{ K}$  and  $C = 1.046 \text{ kJ/kg K}$ ,

$$\dot{Q}_c = 0.48 \left( \frac{\Delta P}{T} \right)^{1/2} \Delta T \quad (9)$$

Accuracy of the operation of the thermocouple array was checked by burning methane gas with known flow rates directly beneath the exhaust collection hood. Comparisons of the results in figure 11 exhibit good agreement between the rates of heat production calculated from the air temperature rise, the oxygen consumption, and the known flow rate of the methane multiplied by its heat of combustion.

#### 3.2.4 Method of Obtaining Rate of Heat Release Per Unit Area of Burning Surface in Model Compartment

Another objective of this study was the measurement of the average rate of heat release per unit area of the burning wall surface within the compartment. Comparison of these measurements with those obtained with the laboratory bench test for the rate of heat release would thus establish the most appropriate exposure conditions in the bench test for providing equivalent room fire test data.

In order to determine the rate of heat release per unit area involved in the compartment, simultaneous measurements of the total rate of heat release and the area involved were made. The area involved was not measured continuously while burning, but was obtained by conducting a number of tests on different wall specimens of the same type of material and extinguishing the flames at various times prior to flashover using a  $\text{CO}_2$  extinguisher. The three combustible walls were removed from the model compartment following each fire test and the burned area was measured.

While the boundary between the areas involved and the areas lightly charred but not burning was not well defined, the surfaces involved scratched easily, whereas surfaces that had not begun to burn remained hard and did not scratch. The areas involved were thus determined by lightly scraping the surface with a sharp-edged tool. A tracing of the boundary was made and the portion of the tracing paper representing the burning area was cut from the overall tracing and weighed. The ratio of this weight to the weight per unit area of the tracing paper was the method used for the area of involvement determinations.

The average heat release rates per unit area were obtained by dividing the total rate of heat production at the termination of the test by the measured area of involvement.

### 3.3 Full-Scale Room Burns -- Details of Room and Exhaust Collection System

The full-scale room burns conducted in this study were primarily intended to demonstrate and confirm the application of the oxygen consumption technique for measuring heat release in full-scale room fires.

To collect the combustion products from the room for the application of the oxygen consumption method of determining heat release, a 1.2 x 1.5 m hood, similar to that used in the model compartment, was constructed and placed above the doorway. It was attached to a pipe 0.2 m in diameter containing a high capacity blower ( $42 \text{ m}^3/\text{min}$ ). The same procedure and instrumentation described previously were used to determine the rate of heat generated.

An ignition source, consisting of a horizontal gas diffusion burner (0.3 x 0.3 m), approximately 16 times the area of the one used in the model compartment, was placed in one back corner of the room opposite the doorway.

The rate of gas flow to the burner was set 16 times higher than that used in the model compartment to produce a flame height approximately one half the height of the wall prior to wall ignition.

The dimensions and layout of the full size room are shown in figure 10, and can be compared with those of the model compartment shown in figure 9. This structure was not an exact 4X scale up of the model compartment. The room had a doorway centered in one wall whereas the model compartment doorway was off center. This difference did not appear to be critical to the overall fire buildup. A significant difference was the unintentional departure from proper scaling of the doorway height which was 1.88 m instead of the scaled 1.78 m height. This reduced the hot gas entrapment distance between the top of the doorway and the ceiling as well as allowing too much airflow. The consequence of the door opening is discussed in section 4.2. The second full-scale room burn was conducted with the correctly scaled doorway height.

#### 4. RESULTS

##### 4.1 Quarter-Scale Model Compartment

###### 4.1.1 Total Heat, Convected Heat, Upper Room Air Temperature, Wall Ignition Time, and Flashover

Three materials--low density wood fiberboard, particleboard, and hardboard--were selected for this study on the basis of having different rates of heat release, densities, and thermal properties, and should therefore result in varying fire development in the model compartment. Each was essentially thermally thick for the preflashover period, and remained in place when burned. The materials were readily available in convenient sheet form. Specimens were installed on three walls of the model compartment; the

wall around the doorway was left unlined. The inner chamber was then balanced on the load cells, and the ignition burner was placed in the corner of the room, within 6 mm of the walls.

The rate of heat produced by the burning walls in the compartment plus the heat from the ignition burner, 2.8 kW, are plotted as a function of time in figures 12 to 14.

Three data points are labeled on the RHR curve indicating the time for a particular occurrence in the compartment--wall ignition time,  $\Delta$ ; specific area involvement,  $X$ ; and flashover,  $0$ . The burner was initially placed arbitrarily within 6 mm of the walls. After obtaining significant variations in the time of wall ignition, it was placed as close as possible without contacting the walls. This resulted in shorter and more uniform ignition times comparable to those obtained by the laboratory test for ease of ignition [13]. See appendix A for comparison of test results of ease of ignition with times for wall ignition.

The  $X$  on each RHR curve is the time required for the  $0.093 \text{ m}^2$  area of the wall directly between the burner and the ceiling to become fully involved. During this time the heat was transferred by direct flame impingement with little additional external radiant heat flux. The flame spread direction was vertically upward during this period of fire development with the zone heated by the flame extending far beyond the pyrolyzing area. To involve more wall area, a transition occurred in the flame spread direction from vertically upward to either lateral from the burning corner or vertically downward from the ceiling. In this case the zone heated by the flame was small and the preheating of the wall surfaces ahead of the flame by external thermal radiation from other heated surfaces and by convective heating had a large effect on the flame spread velocity. These distinctly different conditions of flame spread would be characterized by different modes of heating if comparable conditions were to be duplicated on a laboratory bench scale flame spread test.

The symbol 0 shows the time of flashover, defined in these experiments as the time of ignition of crumpled newspaper on the floor of the compartment; this occurred at a measured mean radiant flux of  $2.6 \pm 0.4 \text{ W/cm}^2$ . The rate of heat release at which room flashover occurred for the three materials examined in the model compartment was  $55 \pm 3 \text{ kW}$ .

Several tests of a model compartment lined with each material were taken to flashover, from which the mean RHR curves plotted in figures 12 to 14 were obtained. Other tests were terminated by extinguishment of the fire with a  $\text{CO}_2$  extinguisher at selected times prior to flashover. The magnitude of the rate of heat release at termination of each model compartment test is plotted as a dot and labeled MC-( ) on the mean RHR curve indicating the number of the experiment. These values were used to determine the rate of heat release per unit area as discussed in section 4.1.2.

Also plotted is the convected heat through the doorway. The ratio of the convected heat (CH) to the rate of heat release (RHR) is approximately 0.5 for each material, being slightly higher for the more thermally insulating fiberboard. A higher ratio means less heat conducted to and through the walls and ceiling and more heat loss through the doorway. The measurement of the temperature rise of the gases entering the stack provides a simpler approach to measuring convected heat through the doorway than the normal method of dividing the doorway into sections and measuring the velocity and temperature at each section. The use of the thermocouple grid in the hood has the advantage of having a known mass flow rate and one whose spatial distribution does not vary as greatly as the one in the doorway.

The third curve in figures 12 to 14 is the simultaneous plot of the upper room air temperature (URT) measured 7.5 cm from the ceiling in the center of the room.

#### 4.1.2 Area and Rate of Heat Release Per Unit Area of Burning Wall at Various Times Prior to Flashover

After termination of each model compartment test, at various times prior to flashover, the three combustible walls were removed and analyzed for area involvement.

Tracings of the boundary between burned areas and non-burned areas for each terminated test are shown in figures 15 to 17. Also included are the area involved and rate of heat release per unit area calculated at the termination time for each test. Since the ignition time of the wall was not constant for each test, due to inconsistent placement distance of the burner from the wall, a corrected termination time is listed. The corrected termination time is the time on the mean RHR vs time curve in figures 12 to 14 corresponding to the last RHR reading from each terminated test.

Also tabulated in the tables in figures 15 to 17 are test results on materials that had been conditioned at 0% RH prior to compartment testing. Flashover for these tests occurred more rapidly, demonstrating that moisture content can significantly alter the results of fire tests. All other materials were stored in an area of near 50% RH prior to compartment testing.

As previously mentioned, one specific purpose of these compartment tests was to determine the average rate of heat production per unit area involved. This should provide insight into the proper use or a more meaningful interpretation of the rate of heat release data from laboratory bench scale tests. Within the compartment, each area element of the wall was exposed to varying exposure conditions and was burning for different lengths of time. This results in substantial differences in the rate of heat release for each area element. The average rate of heat release per unit area was obtained by dividing the rate of heat release by the area burning at the time of measurement.

Significant differences in the rate of heat release per unit area were obtained between the materials tested. The low density fiberboard had a fairly constant and low rate of heat release per unit area of  $6 \text{ W/cm}^2$ . Nevertheless, flashover occurred in the shortest time--3 min 36 sec. The compartments lined with particleboard and hardboard both required longer times--8 min 45 sec and 8 min 53 sec, respectively,--to flashover, even though their rates of heat release per unit area were higher. The particleboard had a fairly constant rate of heat release per unit area of  $9.5 \text{ W/cm}^2$  from full corner involvement to flashover, whereas the rate of heat release for the hardboard is initially  $11 \text{ W/cm}^2$ , increasing to  $16 \text{ W/cm}^2$  at flashover. The fact that the material with the lowest rate of heat release per unit area caused flashover in the compartment in the shortest time emphasizes that the time to ignition and the flame spread rate are also important fire parameters for describing the fire buildup in a room.

#### 4.2 Full-Scale Room Burn

Two full-scale room burns were run to establish a comparison of the average rate of heat release per unit area in the quarter-scale and full-scale room tests. Pictures and observations of the back wall marked with grid lines were taken during the tests in order to determine the area of involvement which is needed for calculating the rate of heat release per unit area. The results from the model compartment and full-scale room burns were in agreement. However, the fire growth in the first full-scale room test, lined with low density fiberboard, was not a duplicate of the model compartment performance. The room doorway was too high to satisfy the scaling rules, as was noted in section 3.3 and did not provide the properly scaled ventilation (airflow) and trapping of the hot gases in the upper part of the room. Consequently, the room did not flash over and the severity of the fire was mild in comparison with the quarter-scale model compartment performance. Details of room and model compartment interior dimensions and door sizes are shown in figures 9 and 10.

The boundary between the involved and non-involved areas for low density fiberboard at various times during the test is plotted in figure 18. From these plots, the burning area was determined. Time, room air temperature 10 cm below the ceiling, area involved, and rate of heat release per unit area are included in the figure. Comparison with the mean rate of heat release per unit area of  $6 \text{ W/cm}^2$  from the model compartment tabulated in figure 15 shows good agreement over the time period from 81 to 138 seconds.

Visual observations of the fire buildup in the room and the model compartment were very similar during the first 2 min 15 sec. After this time, areas which had been burning became extinguished with flaming occurring only at the boundary between burned and unburned areas. Due to the higher airflow and smaller distance from the doorway lintel to the ceiling in the room, the temperatures in the upper part of the room remained lower than that which occurred in the model compartment, providing insufficient heating of the walls to sustain ignition after the char layer had been formed. Consequently, the fire subsided and the test was terminated after 8 min by extinguishment with water from a sprinkler.

Due to the limited availability of the full-scale test room, the fiberboard was removed and the room was immediately relined with 2-ply 6-mm hardboard. The hardboard test was conducted on the following day. The moisture content of the hardboard was probably higher than normal as a result of the elevated relative humidity of the air from the water used to extinguish the fiberboard test.

Properly scaled ventilation (airflow) was provided by lowering the height of the doorway, see figure 10. The exhaust blower for the analysis system was also modified for a higher volume flow to assure complete collection of the combustion products over the whole fire growth period up to flashover.

The corner burner was ignited and after 2 min problems were encountered with the exhaust system. The upper room air temperature had already reached 150°C at which time the gas to the burner was shut off. The room was cooled for one half hour to approximately 30°C while new corner wall panels were installed adjacent to the burner, and the blower motor was changed to prevent another overload. Due to the 150°C temperature encountered in the upper gas layer, the moisture content of the hardboard probably more closely approximated the moisture content of the material conditioned to 0% RH that was tested in the model compartment.

The full-scale hardboard test was restarted and ignition of the wall was first observed at 1 min 30 sec. The boundary between the burning and non-involved areas at various times during the test is shown in figure 19. Also included in this figure are the room air temperature 10 cm below the ceiling, area involved, and the computed rate of heat release per unit area. The first computation of the RHR/area made at 2 min (approximately 1/2 min after the first sign of wall ignition) is low in comparison with the model compartment results, exhibiting a gradually increasing RHR/area as a result of higher radiant flux on the burning surfaces.

During the latter stages of the test, the hood was not able to collect all combustion products due to the limited blower capacity. Consequently, the measured heat release rate after 5 min was low, causing incorrect RHR/area results at flashover.

Since the area of the walls or fuel source of the full-scale room was 16 times that of the quarter-scale model compartment, then 16 times the rate of heat release would be expected to produce the same upper air temperature at identical times if properly scaled. The total rate of heat release from hardboard conditioned at 0% RH and tested in the model compartment and the total rate of heat release from the full-scale test scaled down by a factor of 16 are plotted in figure 20 as a function of the upper room air

temperatures, 2.5 cm from ceiling in model compartment and 10 cm from ceiling in full-scale room. The agreement is striking.

#### 4.3 Laboratory Bench Tests

##### 4.3.1 Rate of Heat Release

Various modes of operation of the laboratory bench test for rate of heat release by  $O_2$  consumption were investigated, each significantly influencing the rate at which heat was produced from the burning materials. These were conducted in order to establish the exposure conditions in the bench test resulting in a mean rate of heat release per unit area the same as that obtained from the model compartment. In order to apply rate of heat release data from the laboratory bench test to describe the buildup in a room, it was desirable that the data be obtained at exposure conditions simulating those in the room as closely as possible. These conditions included the preheat of the walls from the hot upper gas layer and radiation from the surrounding heated surfaces, in addition to direct flame heating and external radiation during the burning period.

These conditions were closely simulated in the bench test by preheating the specimen to a temperature of  $290^{\circ}\text{C}$  using a radiant exposure of  $2 \text{ W/cm}^2$ . An external radiant flux was then applied at levels of 0, 1, 2 and  $3 \text{ W/cm}^2$  and the simultaneous application of a bathing flame from a line pilot burner that produced an additional heat flux of  $3.5 \text{ W/cm}^2$ . The results of these tests are shown in figures 21 to 23 along with the mean rate of heat release per unit area (broken line) obtained in the model compartment tests.

To properly interpret the results from the bench test as they relate to compartment results, the conditions with respect to time within the compartment must be considered. Comparison on an equal time basis is not valid, since the exposure conditions in the bench test were adjusted so that

ignition occurred at or near the time of zero minutes, whereas in the model compartment, ignition occurred at later times. During the early stages of fire growth the only involvement is the corner, directly above the burner. This area is exposed to the bathed flame with little additional heat flux from the surrounding surfaces. The rate of heat release with no external radiation in the heat release rate calorimeter adequately describes the heat released in the room fire during this time for all three materials. Later, the upper room air and surfaces became heated thus exposing burning areas to higher heat fluxes. These higher heat fluxes cause higher rates of heat release unless the time for which the surface has been burning is on the decreasing portion of the curve for rate of heat release. Both the fiberboard and the particleboard exhibit a peak rate of heat release followed by a gradually decreasing rate. Areas that have been burning for some time at low additional heat fluxes show decreasing rates of heat release. It is speculated that burning areas that continue to receive gradually increasing heat fluxes produce nearly constant heat outputs, while other areas just becoming involved produce heat outputs higher than the mean. The mean heat release rate per unit area from all of the burning areas remains nearly constant at  $6 \text{ W/cm}^2$  for fiberboard and  $9.5 \text{ W/cm}^2$  for particleboard throughout the model compartment burn duration.

The curves for the rate of heat release for hardboard exposed to a constant flux do not exhibit a peak followed by a gradual decrease with time, but more nearly a plateau. The rate of heat release per unit area from hardboard in the model compartment is initially  $11 \text{ W/cm}^2$  and increases to  $16 \text{ W/cm}^2$ .

The rate of heat release curves from the bench test are not extended to the time to flashover because none of the area involved in the model compartment has burned for that duration. In fact the maximum duration of burn of any area is from ignition to flashover with the major portion of the involved area at flashover becoming ignited after full corner involvement.

The time between full corner involvement and flashover, labeled X and 0 respectively in figures 12 to 14, is the basis used for defining the mean RHR curves from the model compartment shown in figures 21 to 23.

A comparison of the mean heat release rate at each exposure condition in figures 21 to 23 indicates that the rate of heat release for all three materials tested in the model compartment may be approximated on the bench test by exposure to a bathed flame with no external radiation initially, increasing to  $1 \text{ W/cm}^2$  at a time comparable to the time duration from full corner involvement to flashover.

#### 4.3.2 Flame Spread

The results of section 4.1.2 demonstrate no direct relationship between rate of heat release per unit area and the time to flashover. Other fire parameters must also be important to adequately describe the severity and rate of buildup of a room fire. One such parameter is the flame spread rate which determines the rate of area involvement.

In the model compartment the flames from the fire source impinge upon and then involve a portion of the wall after heating it to its pyrolysis temperature. The additional fuel generation causes the flames to extend and then the pyrolyzing area increases causing further flame extension until the entire area directly between the burner and the ceiling is burning and the flames are extending along the wall/ceiling intersections. Beyond this time, the exposure conditions for further wall area involvement become quite different. To involve more area the flame must propagate in directions either perpendicular to or opposite to the fire plume flow, that is, lateral or downward. The additional wall surfaces that become involved are convectively preheated by the hot, upper gas layer and radiatively preheated by the other high temperature surfaces rather than by the direct fire plume impingement. Flame contact, however, still supplies the heat needed to bring

the surface from the preheat to the pyrolysis temperature. If there is little heat trapped in the upper room further spread of the flame will be minimal and the conditions of an open corner fire test would be closely simulated. However, if a sufficiently high upper room air temperature is obtained, the flames will spread downward and laterally involving additional surface area until the rate of heat release becomes sufficient to flash over the room.

To simulate the flame spread on the model compartment walls during the latter stages of fire growth resulting in flashover, lateral flame spread tests on a vertical surface were conducted. Vertical specimens 7.5 cm high x 30 cm long were exposed to various levels of radiant heat flux with the simultaneous application of a vertical line pilot burner at one end of the specimen.

The flame propagation distance was measured as a function of time (figures 24 and 25). The average surface temperatures of the non-burning area ahead of the flame front were measured with surface applied thermocouples and are recorded on each curve. The slope of these curves or rate of flame spread was computed and plotted in figure 26 as a function of the surface temperature.

For a semi-infinite solid exposed to a constant heat flux,  $H$ , the rise in surface temperature is given by classical heat conduction theory [14] by

$$T - T_o = \frac{2}{\sqrt{\pi}} \frac{H\sqrt{t}}{\sqrt{\lambda\rho C}} \quad (10)$$

If the preheating region ahead of the pyrolysis zone of a thermally thick combustible solid has an effective length  $\ell$  and an average rate of heat transfer  $H$ , the time to heat the surface from  $T_s$  at the leading edge of this region to the pyrolysis temperature  $T_p$  is given by

$$t = \frac{\pi}{4} \frac{\lambda\rho C}{H^2} (T_p - T_s)^2$$

and the flame spreading velocity is

$$v_f = \frac{\ell}{t} = \frac{4\ell H^2}{\pi \lambda \rho C} \frac{1}{(T_p - T_s)^2} = \frac{F}{(T_p - T_s)^2} \quad (11)$$

where  $\lambda$ ,  $\rho$ , and  $C$  are the thermal conductivity, density, and heat capacity of the solid, and  $F$  is assumed to be characteristic of the material.

It was verified that for hardboard and fiberboard (particleboard was not tested) the rate of flame spread could be expressed by this equation. This was accomplished by conducting a nonlinear regression analysis where the solution represented by the X's in figure 26 indicates a good fit. The  $T_p$  for both materials was determined to be nearly identical at 350°C, which is a reasonable approximation of the pyrolysis temperature of cellulose. The proportionality constant  $F$  was found to be 3310 for fiberboard and 800 for hardboard when the flame spread rate is expressed in meters per min or 55 and 13.3, respectively, when the flame spread is expressed in m/s. The ratio of these proportionality constants indicates that the relative flame spread rate for fiberboard is approximately four times that of hardboard at equivalent surface temperatures. The  $F$  can be considered to be a characteristic of the lateral flame spread rate of a material on the wall and might be used as one of the parameters needed to predict fire buildup in a compartment.

#### 4.4 Comparison of Heat of Combustion With Effective Heat of Combustion

The effective heat of combustion of many solid materials differs significantly from their actual net heat of combustion. To demonstrate these differences, effective heats of combustion were obtained in the model compartment and in the bench test for rate of heat release and compared to the actual net heat of combustion obtained with the oxygen bomb calorimeter. The results are shown in table 2.

Formation of char in a pyrolyzing solid which was not burned in these tests reduces the heat of combustion during the flaming phase. This does not occur in the oxygen bomb calorimeter which consumes the char. This is at least part of the reason for the 20 to 40 percent difference between the effective net and actual net heats of combustion.

The differences in the bench test and model compartment results are partly attributable to moisture in the model compartment being vaporized from heated surfaces that are not burning. This increases the rate of weight loss which in turn lowers the apparent effective net heat of combustion.

## 5. RATIONALIZATION OF OBSERVED FLASHOVER TIMES IN MODEL COMPARTMENT

Ignition, flame spread rate, and heat release rate of combustible wall linings all influence the rate of fire buildup in a room, ultimately leading to a condition necessary for flashover. Each of these fire phenomena has been quantified by measurements taken on laboratory bench tests, at exposures approximating the conditions attained in the model compartment. Using each of these properties is essential to evaluate a material's performance in the model compartment.

The rate of heat release from the burning walls of the compartment at any time is equal to the product of the area of involvement at that time and the average heat release rate per unit area. This can be expressed as follows.

$$\dot{Q} = \dot{q} L v_F t$$

where  $\dot{q}$  = mean rate of heat release per unit area, ( $\text{kW/m}^2$ ),

$L$  = length of the boundary between burning and non-burning area, (m),

$v_F$  = flame spread rate, (m/s), and

$t$  = time (s)

Note that  $L$  and  $v_F$  are average values over time  $t$ .

The time difference  $t^*$  from wall ignition  $t_{ig}$  to flashover  $t_{fo}$  is the time necessary to produce a critical rate of heat release and upper room air temperature necessary for flashover. The critical rate of heat release,  $\dot{Q}^*$ , at which the compartment used in this study flashed over was measured to be 55 kW for the three materials examined (see section 4.1.1). In terms of the critical rate of heat release,

$$t^* = t_{fo} - t_{ig} = \frac{\dot{Q}^*}{\dot{q} L v_F} \quad (12)$$

Combining equations 11 and 12 it is possible to express the flashover time  $t_{fo}$  in terms of the time to ignition, the average heat release rate, and a characteristic flame spread constant,

$$t_{fo} = t_{ig} + \frac{\dot{Q}^* (T_p - T_s)^2}{L} \left( \frac{1}{\dot{q}} \cdot \frac{1}{F} \right) = t_{ig} + \frac{C_4}{\dot{q} F} \quad (13)$$

Actually  $T_s$  is a function of time but equation 13 is based on the assumption that there is a characteristic surface temperature just ahead of the flame as it moves across the surface. Substitution of the experimental data of  $t_{ig}$  and  $t_{fo}$  from the model compartment and  $\dot{q}$  and  $F$  from the bench tests into this expression results in an empirical value for  $C_4$  which is nearly the same for both materials as seen in table 3.

It can be seen, however, from the expansion of  $C_4$  in equation 13 that it would be expected to be strongly scale dependent through  $L$  and  $\dot{Q}^*$ , and material dependent through  $T_p$ . It is also somewhat insulation dependent through  $\dot{Q}^*$ , (since a reduction in heat losses through the walls results in a lower required heat release rate to produce flashover).

Even though only two materials were evaluated, it appears plausible that this same constant  $C_4$  may be applicable to other materials having the same  $T_p$

if evaluated in like manner. This rationalization suggests a conceivable approach for applying bench test results to determine a fire hazard rating for interior finish materials.

## 6. SUMMARY

1. A technique was developed to determine the rate of heat produced from a fire by measuring the rate of oxygen consumed. The principle utilized for this determination is that for a given volume of oxygen consumed there is associated a fixed amount of heat produced of  $16.7 \text{ MJ/m}^3$ . It was verified on a laboratory bench scale test using a known flow rate of methane that this technique has an accuracy of  $\pm 10$  percent when the composition of the burning material is known. Taking into account the differences in heat released per volume of oxygen consumed the accuracy is  $\pm 15$  percent for unknown materials of concern in the room fire environment. The rates of heat release are comparable when determined by oxygen consumption and by calorimetric methods. The technique was demonstrated to be versatile in application to various burning situations including a laboratory bench test for heat release rate, a reduced-scale model compartment fire test, and full-scale room burns.

2. A quarter-scale model compartment was designed to evaluate the contribution of wall linings to room fires in which the walls could be continuously weighed during the fire with a sensitivity of a few grams. The rate of weight loss in conjunction with the rate of heat release from the compartment walls permits computation of the effective heat of combustion in a simulated fire situation.

3. The laboratory bench test for determining the rate of heat release was equipped with a load cell to simultaneously measure heat release and weight loss rates in order to obtain the effective heat of combustion. The effective heats of combustion measured in the model compartment were similar

to those obtained in the bench RHR tests, but both were significantly lower (20-40%) than the net heat of combustion determined by the oxygen bomb calorimeter.

4. Utilization of the model compartment permitted accurate computation of the rate of heat release per unit area involved in a dynamic fire situation. Comparison with the laboratory bench test for the rate of heat release operated in various modes established that the heat release rates are similar when the bench test exposure conditions include a bathed flame exposure with additional thermal radiation of 1 W/cm<sup>2</sup>.

5. A thermocouple grid at the entrance to the stack along with mass flow rate measurements with a thermocouple and pitot-static tube downstream of the grid was set up to measure the heat convected through the doorway of the model compartment. Subtracting this heat from the total heat produced gives the heat lost through the walls, ceiling, and floor of the compartment. This method should prove to be valuable in checking the energy balance when an analytical model is developed to predict fire growth in a room.

6. It was verified that for hardboard and fiberboard the lateral flame spread rate on a vertical surface could be expressed by the equation  $v_F = \frac{F}{(T_p - T_s)^2}$ . The proportionality constant F is defined as the characteristic flame spread constant for a material. The constant values of F for fiberboard and hardboard are 55 and 13.3, respectively, when the flame spread rate is expressed in meters per second. This indicates a flame spread ratio of approximately 4 for these two materials at equivalent surface temperatures.

7. The heat release rate of interior finish materials when considered separately is not a suitable indicator for estimating flashover times in a room fire. It was shown that wall ignition time is related to the time to

ignition in the ease of ignition test and that the time from wall ignition to flashover in a compartment lined with combustible walls is inversely proportional to the product of the rate of heat release and the characteristic flame spread constant  $F$ .

## 7. RECOMMENDATIONS

1. Research should be continued in the further development of a bench test for the rate of heat release and the effective heat of combustion using the oxygen consumption technique along with a continuous rate of weight loss measurement using a load cell. This technique is accurate, versatile, and is less expensive than other methods. In addition to its predictive power for room fires it could serve as an economical method for evaluating flame retardant treatments.

2. A flame spread test should be further developed in which the horizontal flame spread rate along a vertical surface is measured as a function of the temperature of the surface ahead of the flame. The data from such a test along with the data from suitable laboratory tests for heat release rate and time to ignition can potentially be used to predict the time to flashover in a room.

3. The oxygen consumption method should be used as a standard technique for measuring the rate of heat release in large-scale room fire tests for interior finish and furnishing materials. The conventional method of measuring the rate of weight loss and multiplying by the heat of combustion has some difficulties. It is usually not practical to weigh the walls of a full-scale room, and, in the case of burning furniture, there are usually several different materials burning with different and unknown heats of combustion. Furthermore, the heat of combustion which is measured with the oxygen bomb calorimeter can, at least for cellulosic fuels, be considerably higher than the effective heat of combustion which should be applied during large-scale fires.

4. Equipment utilizing the oxygen consumption concept for measuring the rate of heat production from burning materials could be applied to a variety of other tests, such as the flooring radiant panel, the fire endurance test for wall and floor/ceiling assemblies involving combustible constructions, and the ASTM E 84 tunnel test.

5. The calorimetric methods presently used to determine the heat release rate of materials depend on the temperature rise of the stack gases. If the flames from the specimens are highly luminous an appreciable part of the heat may be radiated away before it reaches the measuring point in the stack. If the walls are well insulated most of this heat will eventually be picked up and measured but the shape of the heat release rate versus time curve will be distorted. There has been no systematic study of the magnitude of this error for interior finish materials. The oxygen consumption method of measuring the heat release rate (which is not affected by heat losses) could be used to compare the results of these two methods to examine the effect of heat losses in the existing calorimeters.

#### 8. ACKNOWLEDGMENTS

The author is indebted to those at Armstrong Cork Company responsible for making possible my year as a Research Associate at the National Bureau of Standards where this research was conducted. My gratitude goes to Hank Roux, Armstrong, for his guidance and to individuals of the Center for Fire Research who expressed interest in this work by assisting, by supplying needed instrumentation, and by the encouragement and guidance through helpful discussions. In particular, I wish to thank Bill Parker who was most instrumental in the success of this research effort. His expertise and devotion to fire research were an inspiration. Critical to this research effort was data reduction. For this I am greatly indebted to Jim Jackson, Armstrong, who wrote the necessary programming and processed the data.

I would like to express my gratitude to the CFR readers, D. Gross, W. Parker, B. Lee, C. Huggett, A. Robertson, and V. Babrauskas, who reviewed this report and for their very useful comments.

## 9. REFERENCES

- [1] Standard method of test for surface burning characteristics of building materials, ASTM E 84-79a, American Society for Testing and Materials, Philadelphia, Pa. (1979).
- [2] Fang, J. B., Fire buildup in a room and the role of interior finish materials, Nat. Bur. Stand. (U.S.), Tech. Note 879 (June 1975).
- [3] Parker, W. J. and Long, M. E., Development of a heat release rate calorimeter at NBS -- Ignition, heat release, and noncombustibility of materials, ASTM STP 502, American Society for Testing and Materials, 135-151 (1972).
- [4] Smith, E. E., Heat release rate of building materials -- Ignition, heat release, and noncombustibility of materials, ASTM STP 502, American Society for Testing and Materials, 119-134 (1972).
- [5] Parker, W. J., An investigation of the fire environment in the ASTM E 84 tunnel test, Nat. Bur. Stand. (U.S.), Tech. Note 945 (August 1977).
- [6] Huggett, C., Oxygen Consumption Calorimetry, Proceedings Eastern Section of the Combustion Institute, 1978 Fall Technical Meeting.
- [7] Jessup, R. S. and Prosen, E. J., Heats of combustion and formation of cellulose and nitrocellulose (cellulose nitrate), Nat. Bur. Stand. (U.S.), J. 44, 387-393 (1950).
- [8] Handbook of Chemistry and Physics, 57th Edition, CRC Press (1976-1977).
- [9] Loftus, J. J., Gross, D. and Robertson, A. F., Potential heat -- A method of measuring the heat release of materials in building fires, Proceedings of the ASTM, Philadelphia, Pa., Vol. 61 (1961).
- [10] Evans, D. D. and Breden, L. H., Time delay correction for heat release rate data, Fire Technology, Vol. 14, No. 2, 85-96 (May 1978).
- [11] Parker, W. J. and Lee, B. T., Fire buildup in reduced size enclosures, Nat. Bur. Stand. (U.S.), Special Publication 411 (November 1974).
- [12] Waterman, T. E., Room flashover -- Model studies, Fire Technology, 316-325 (November 1972).
- [13] Lawson, J. R. and Parker, W. J., Development of an ease of ignition test using flame impingement, Nat. Bur. Stand. (U.S.), NBSIR to be published.
- [14] Carslaw, H. S. and Jaeger, J. C., Conduction of Heat in Solids, Second Edition, Oxford University Press, p. 75 (1959).
- [15] Baumeister, T., Editor, Mark's Standard for Mechanical Engineers, Seventh Edition, 4-72 (1967).
- [16] Fang, J. B. and Breese, J. N., Fire development in residential basement rooms, Nat. Bur. Stand. (U.S.), NBSIR to be published.

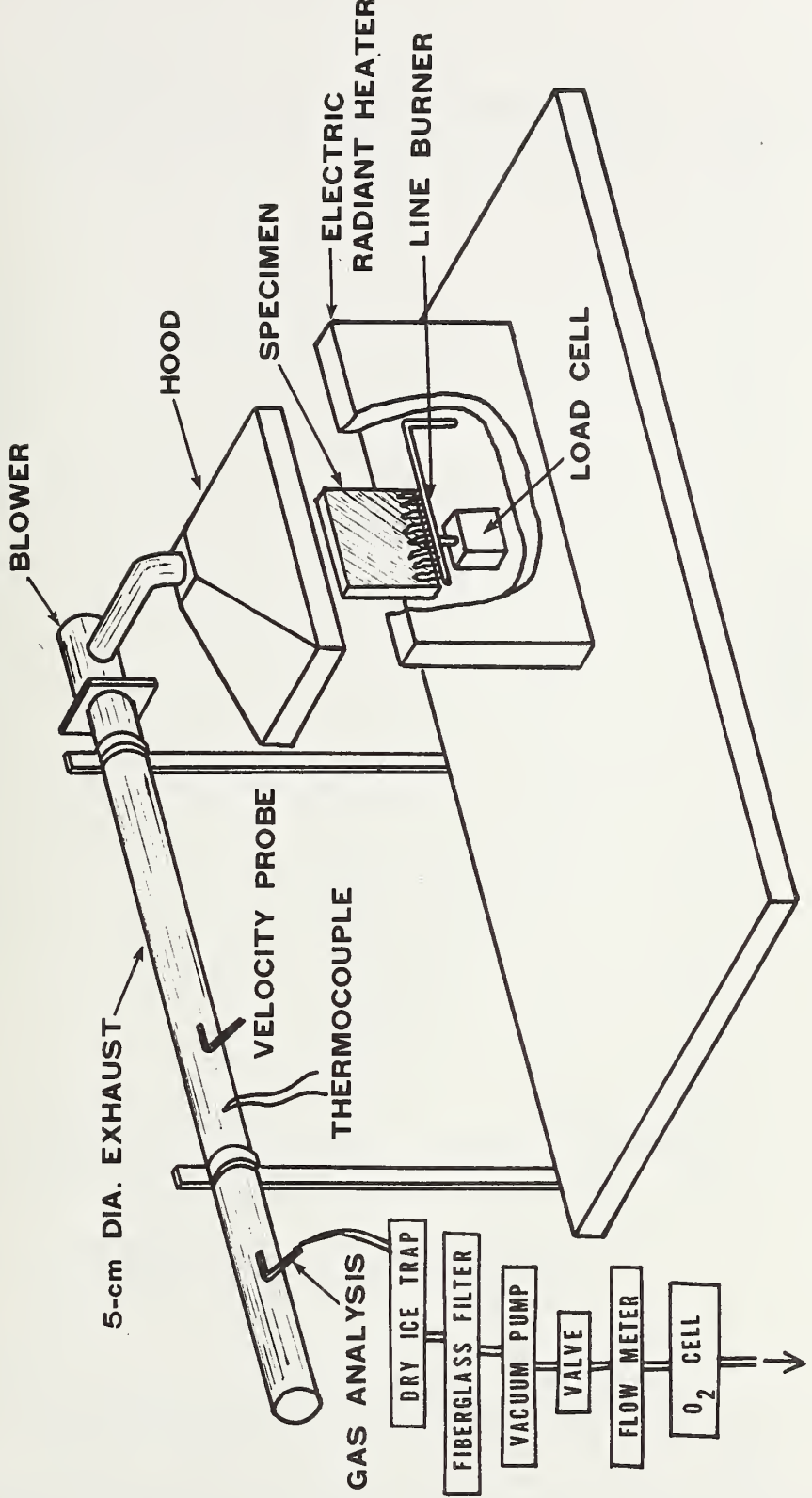


Figure 1. Apparatus for measuring rate of heat release by oxygen consumption

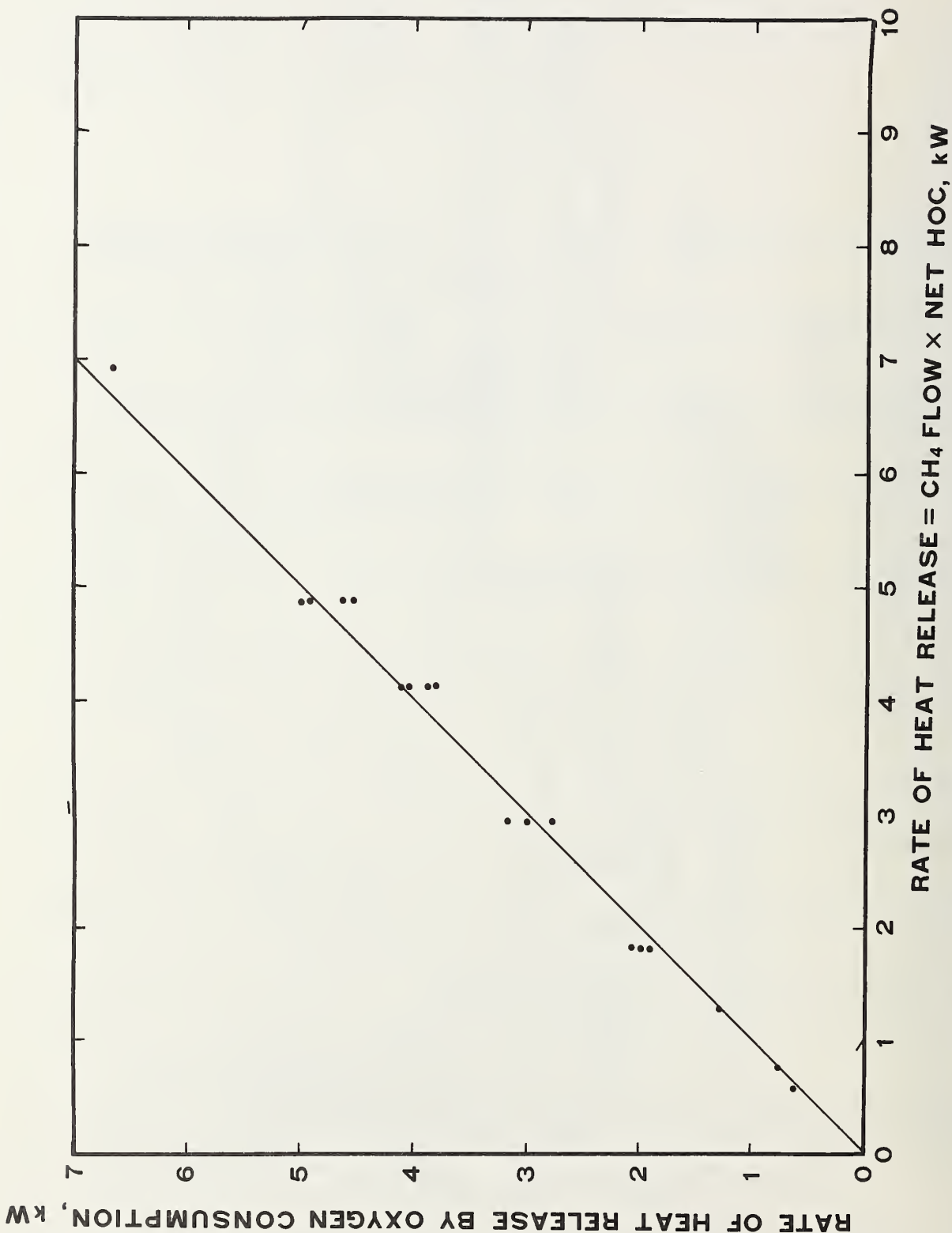


Figure 2. Comparison of the rate of heat release from burning methane of known heat of combustion (HOC) at various flow rates with rate of heat release by oxygen consumption

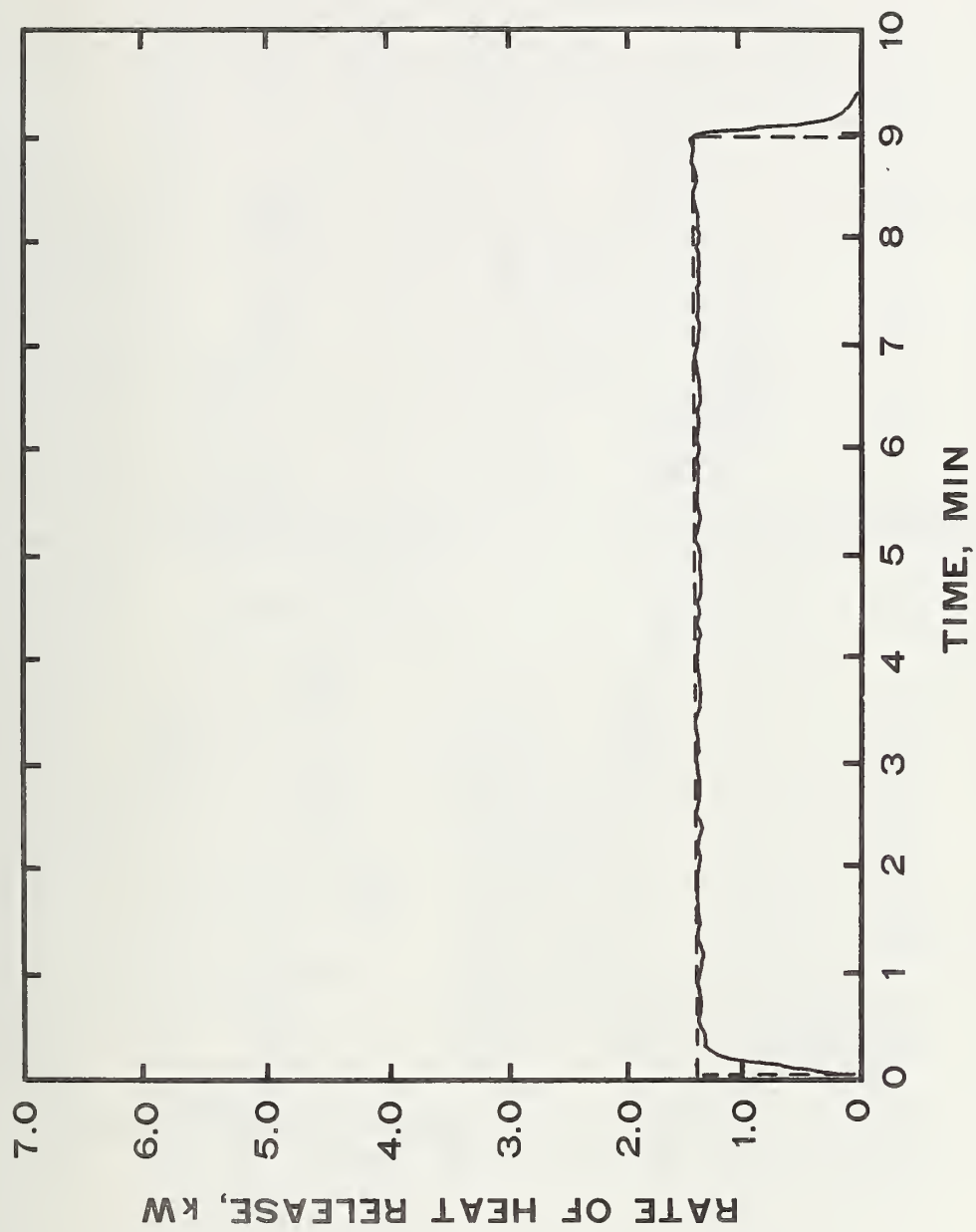


Figure 3. Comparison of the rate of heat release from burning methane at a flow rate of 2.53 l/min (1.43 kW) with rate of heat release by oxygen consumption

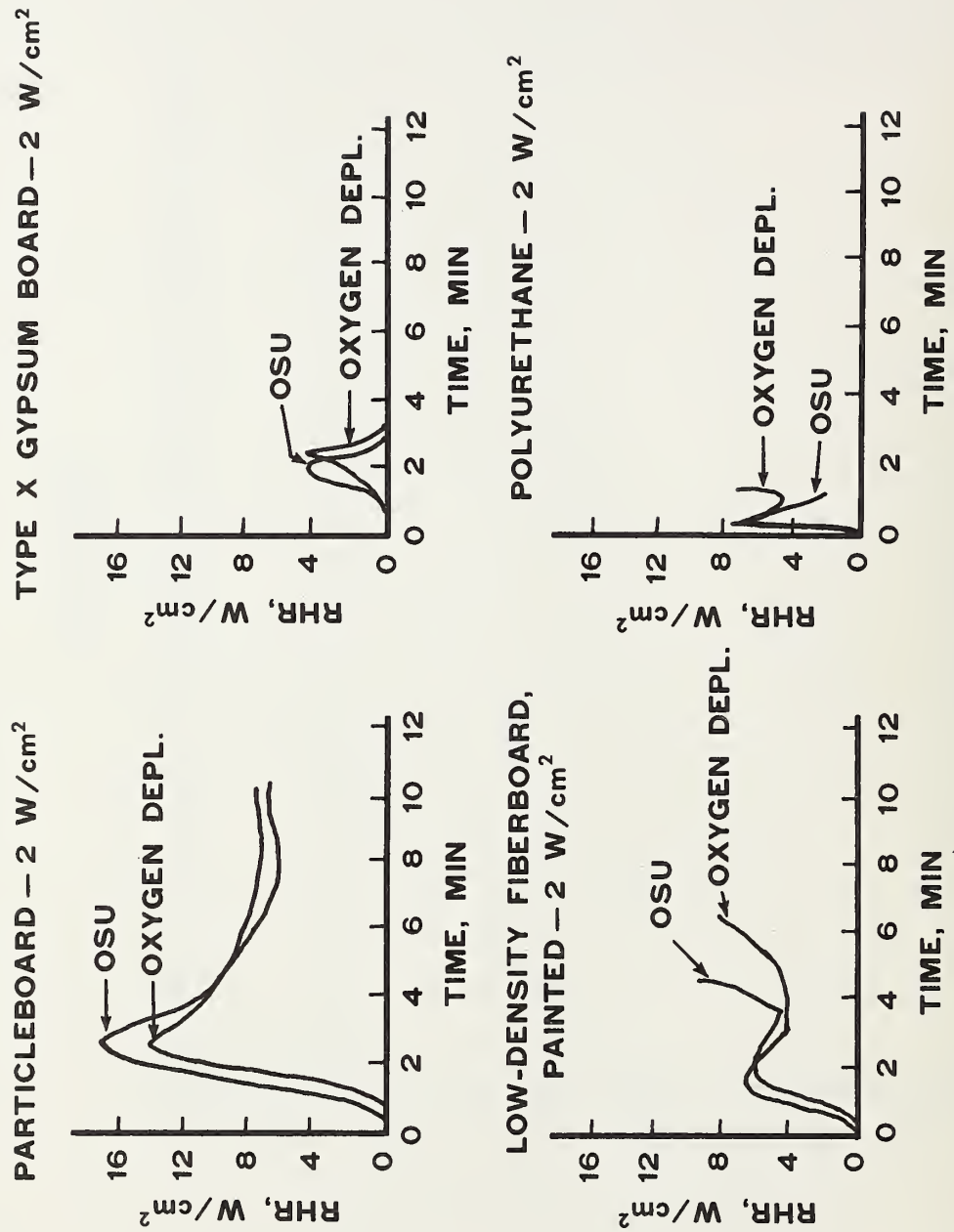


Figure 4. Rate of heat release -- Ohio State calorimeter and oxygen consumption bench test comparison

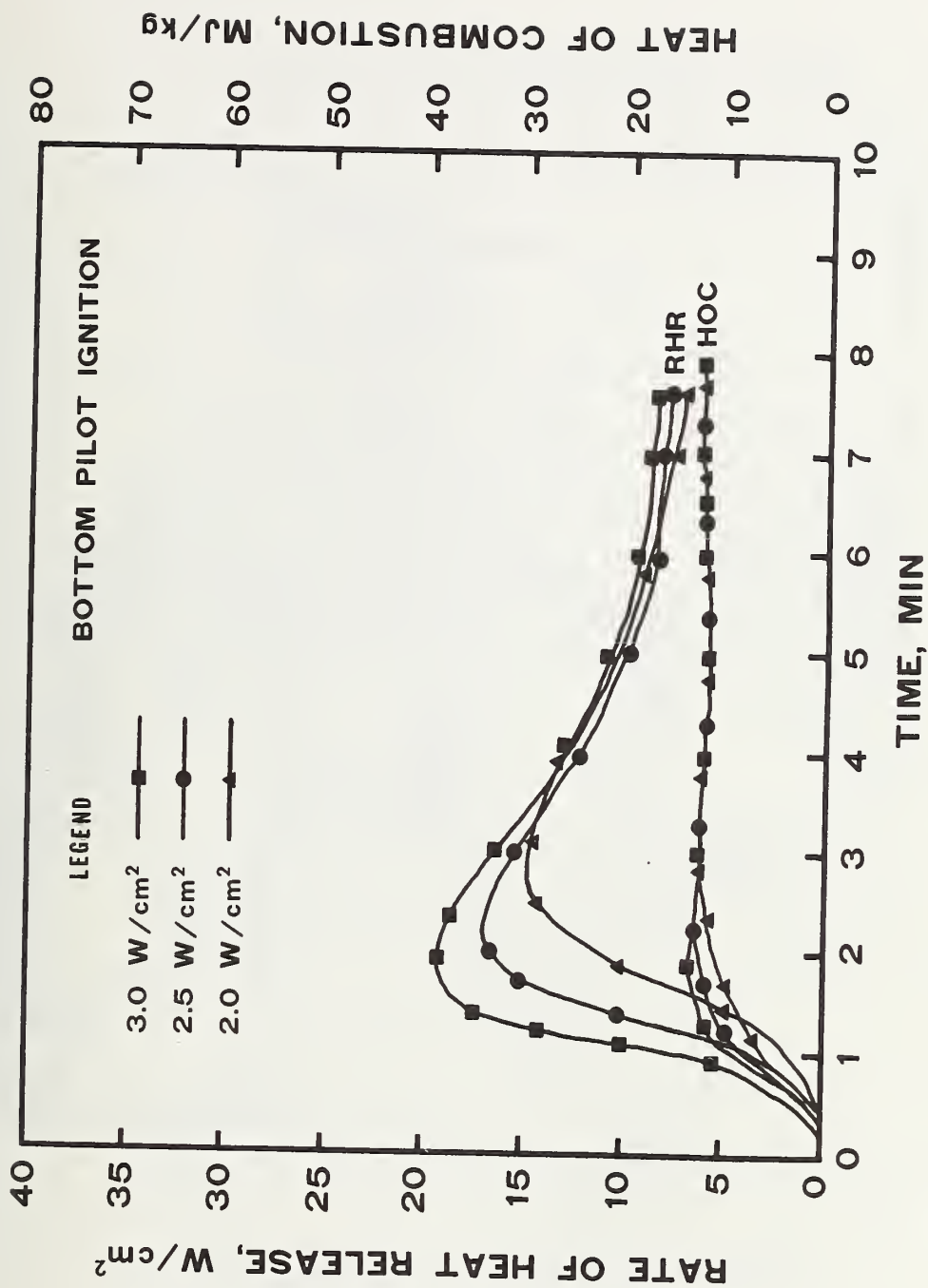


Figure 5. Rate of heat release and effective heat of combustion of 16-mm particleboard (~50% RH) -- bench test results

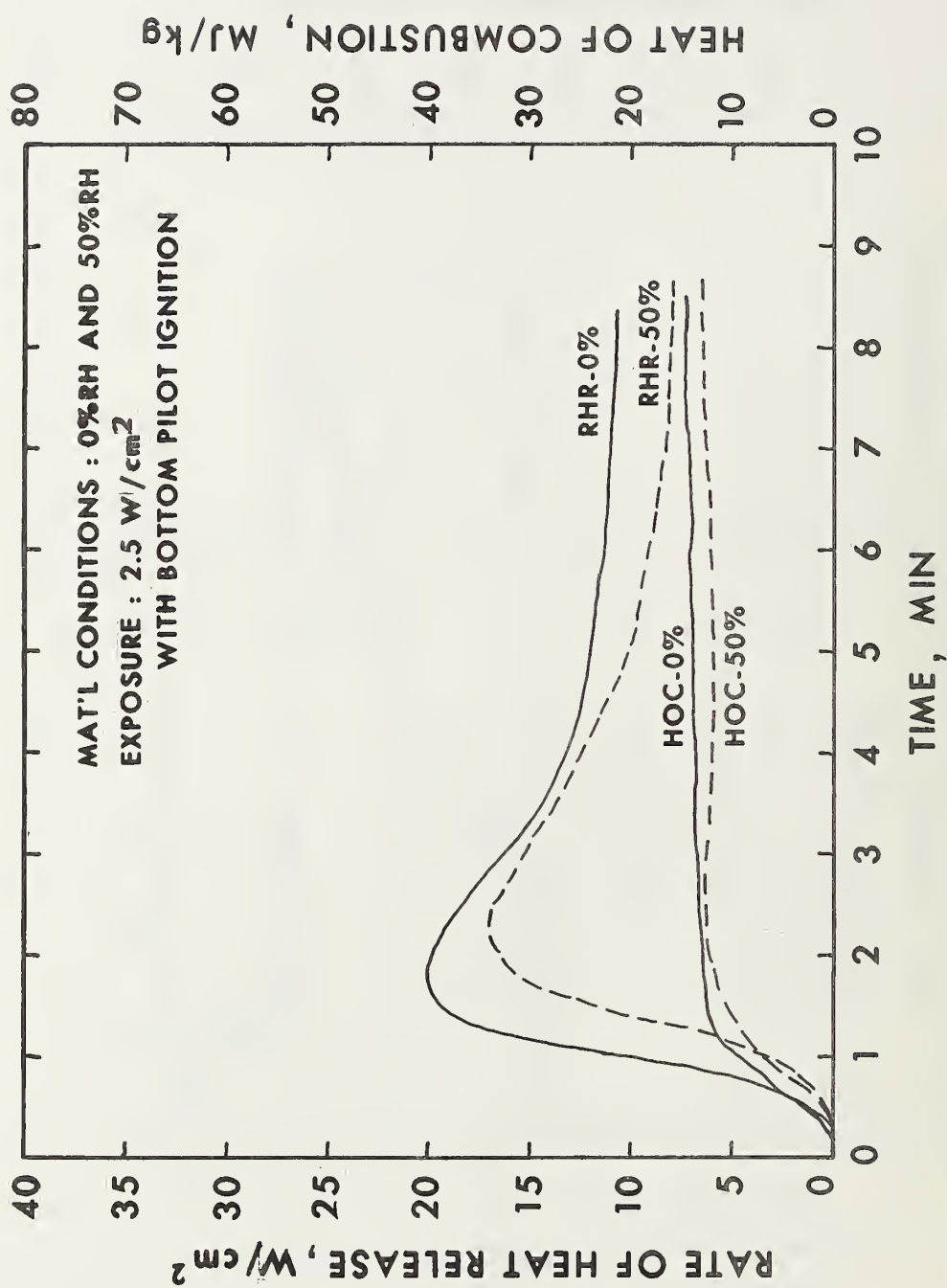


Figure 6. Rate of heat release and effective heat of combustion of 16-mm particleboard at 0% and 50% RH -- bench test results

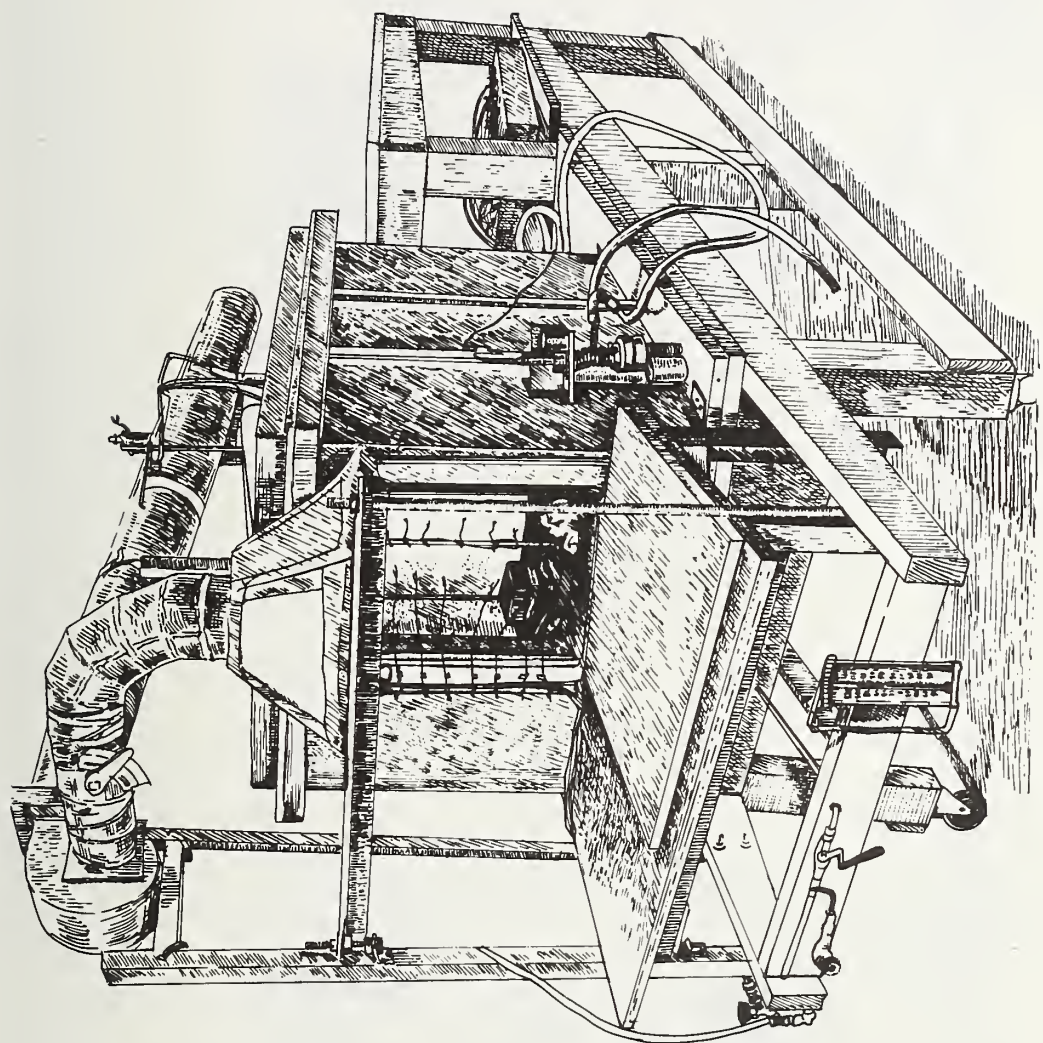


Figure 7. Model compartment -- sketch

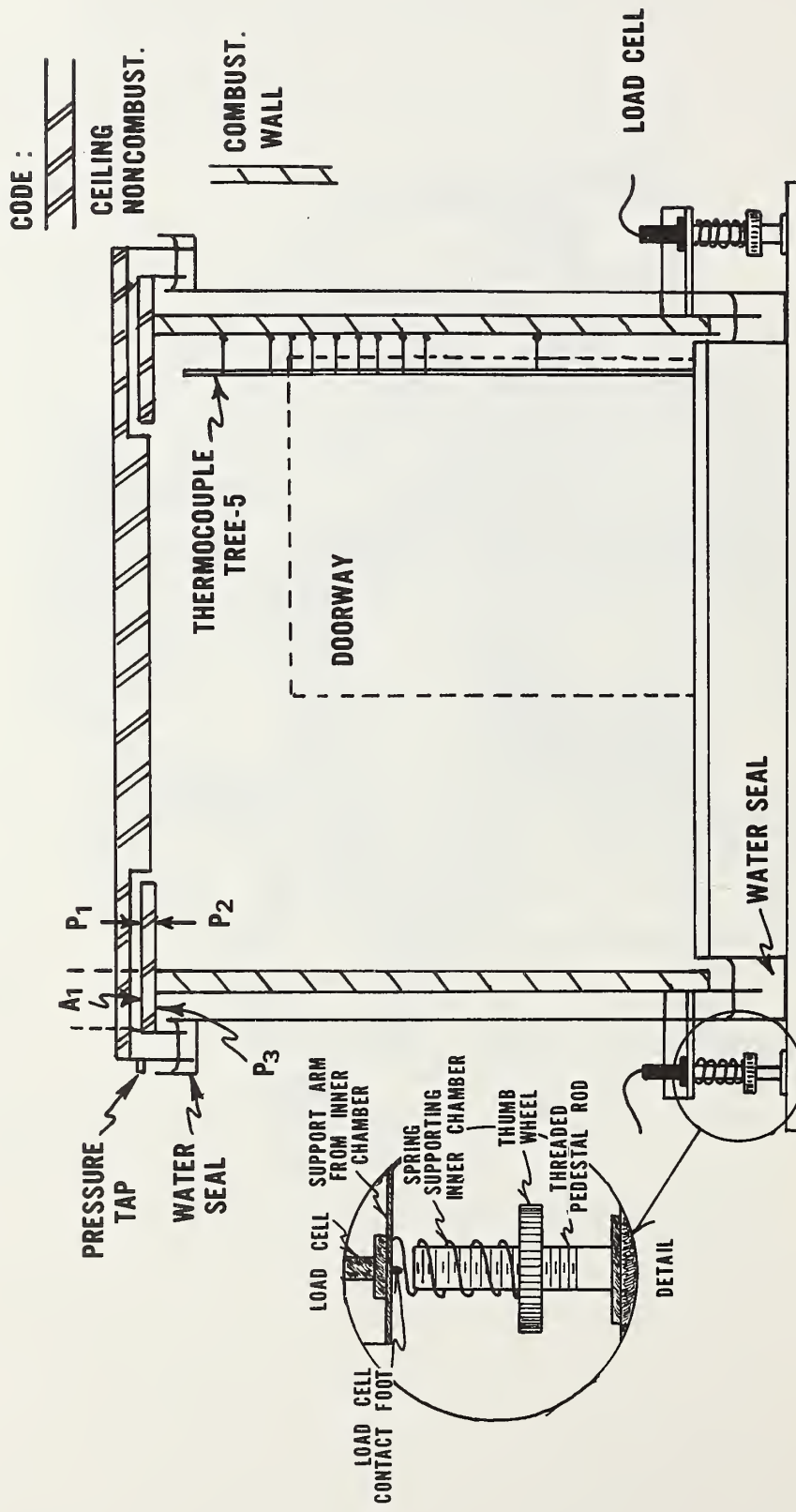


Figure 8. Model compartment -- cross section

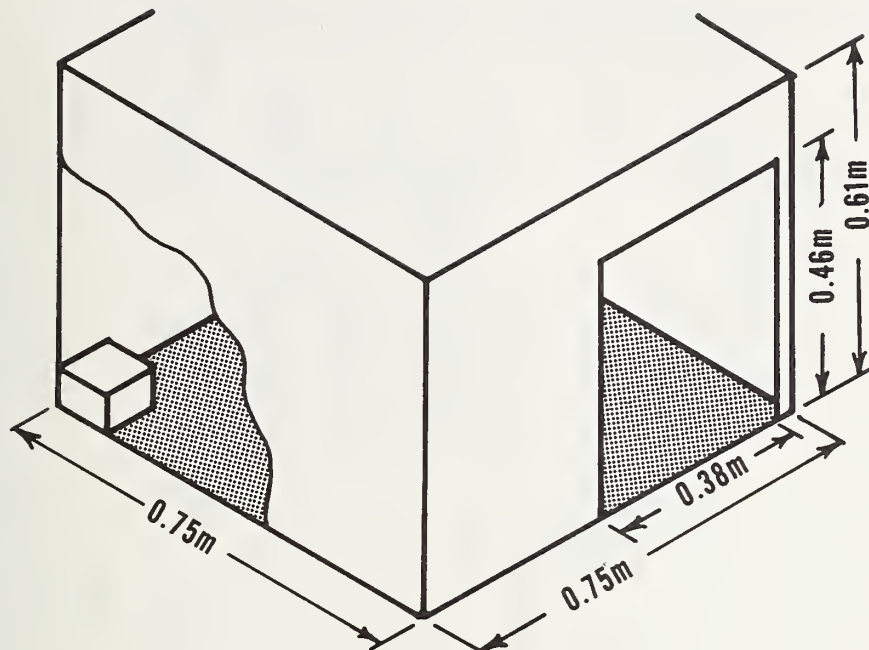


Figure 9. Quarter-scale model compartment

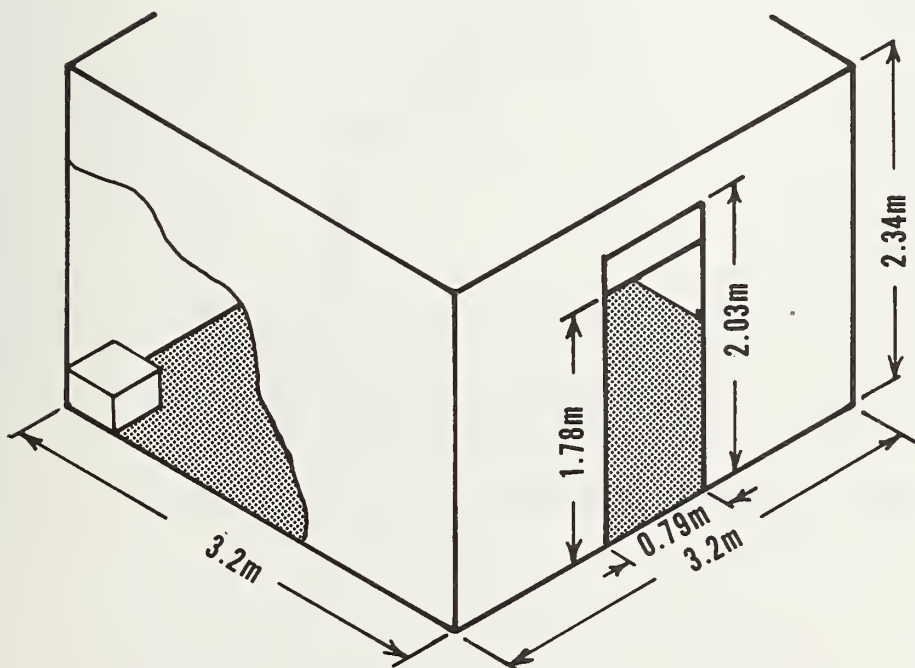


Figure 10. Full size room

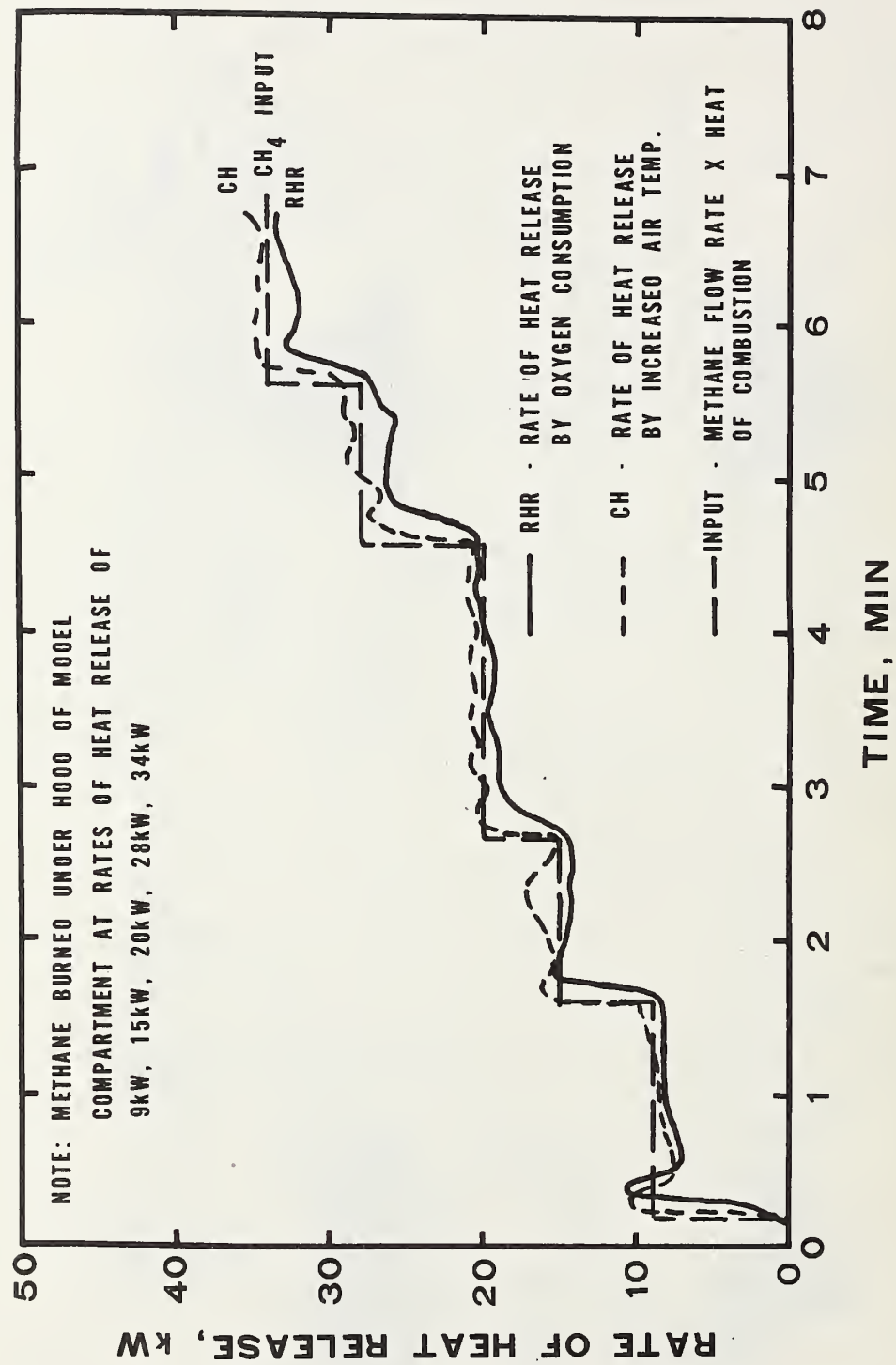


Figure 11. Comparison of convected heat into hood with total rate of heat release measured by oxygen consumption from burning methane at various rates of heat release

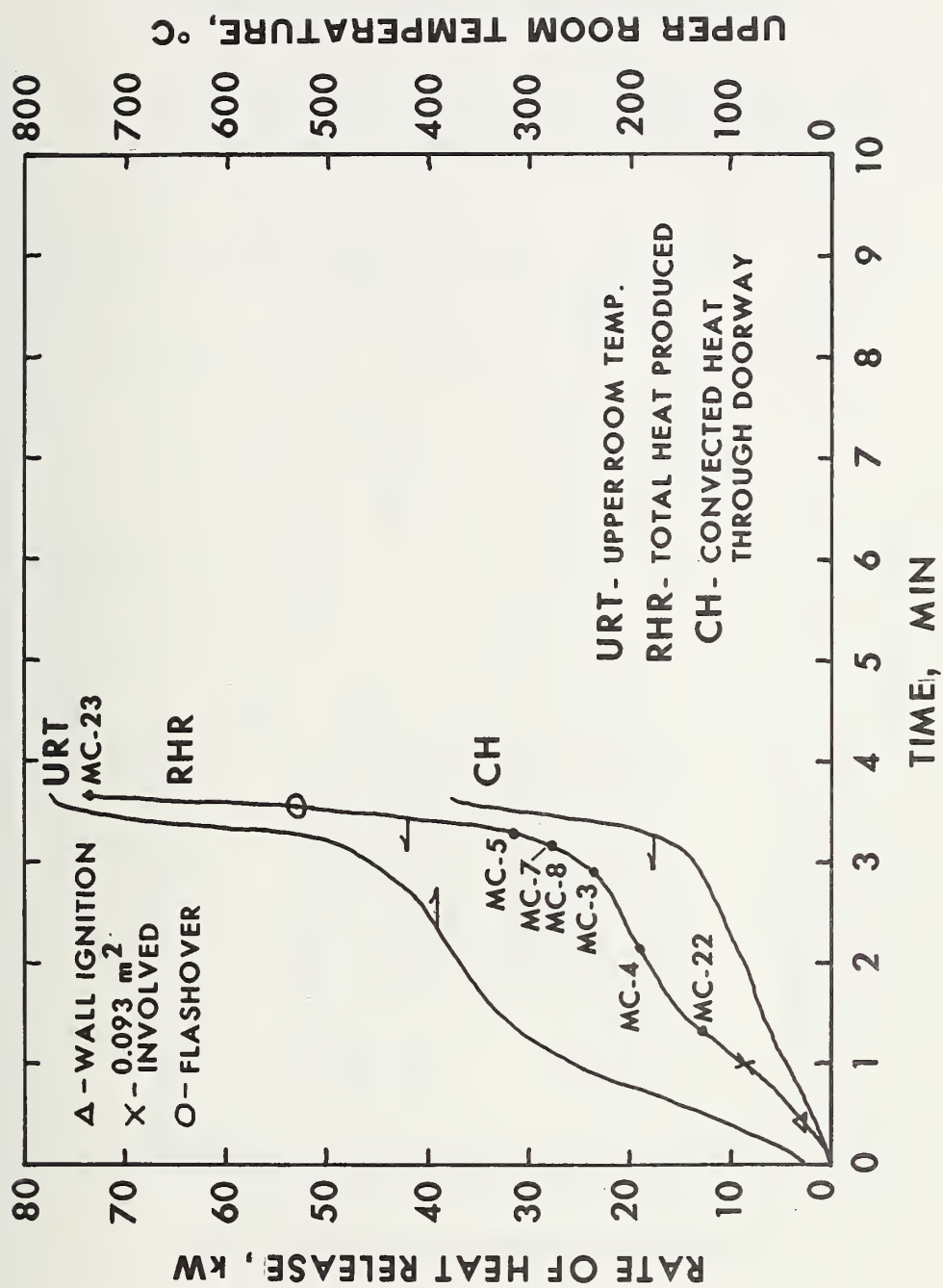


Figure 12. Model compartment results -- 12-mm low density wood fiberboard

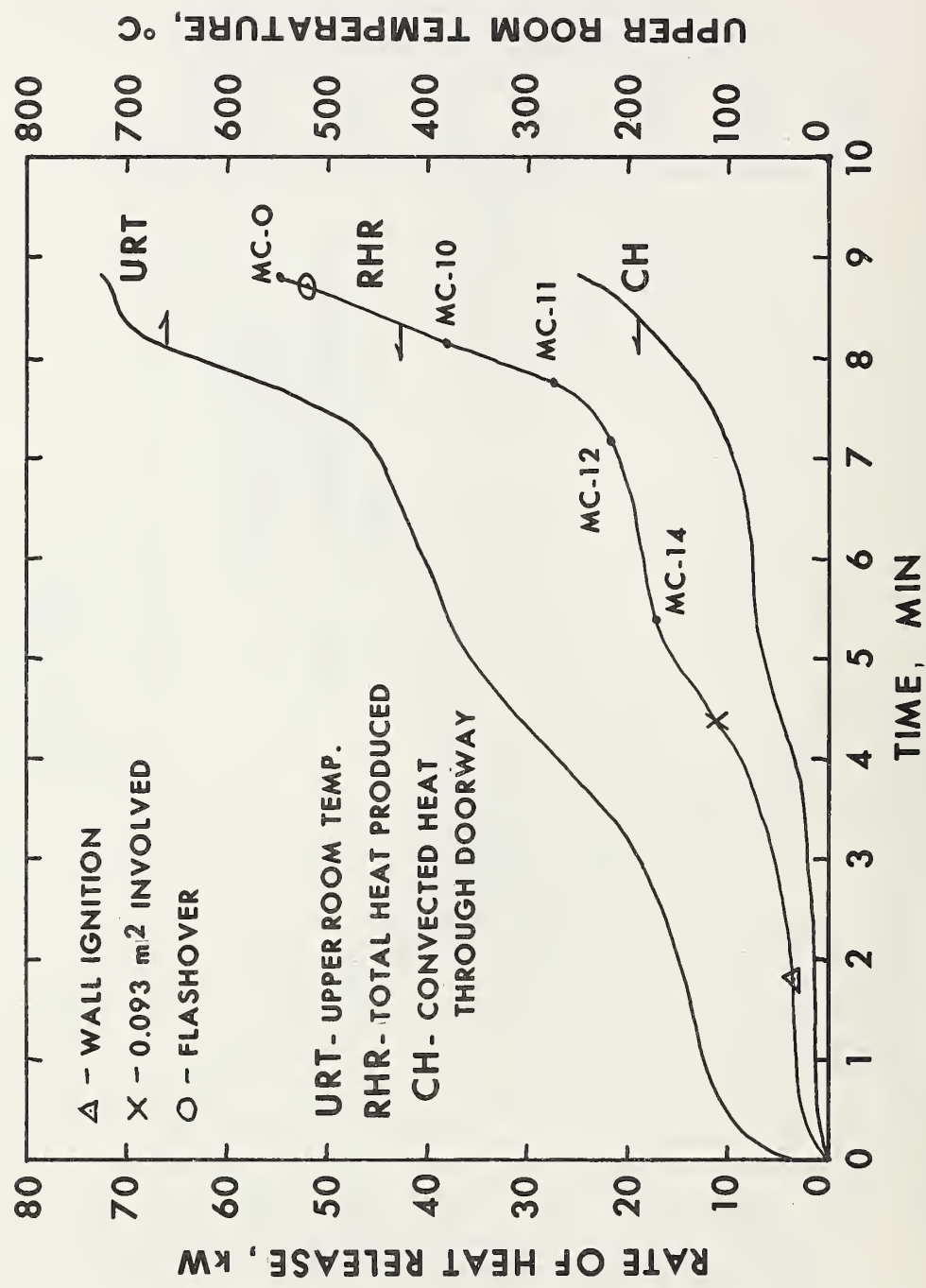


Figure 13 Model compartment results - 16-mm insulation

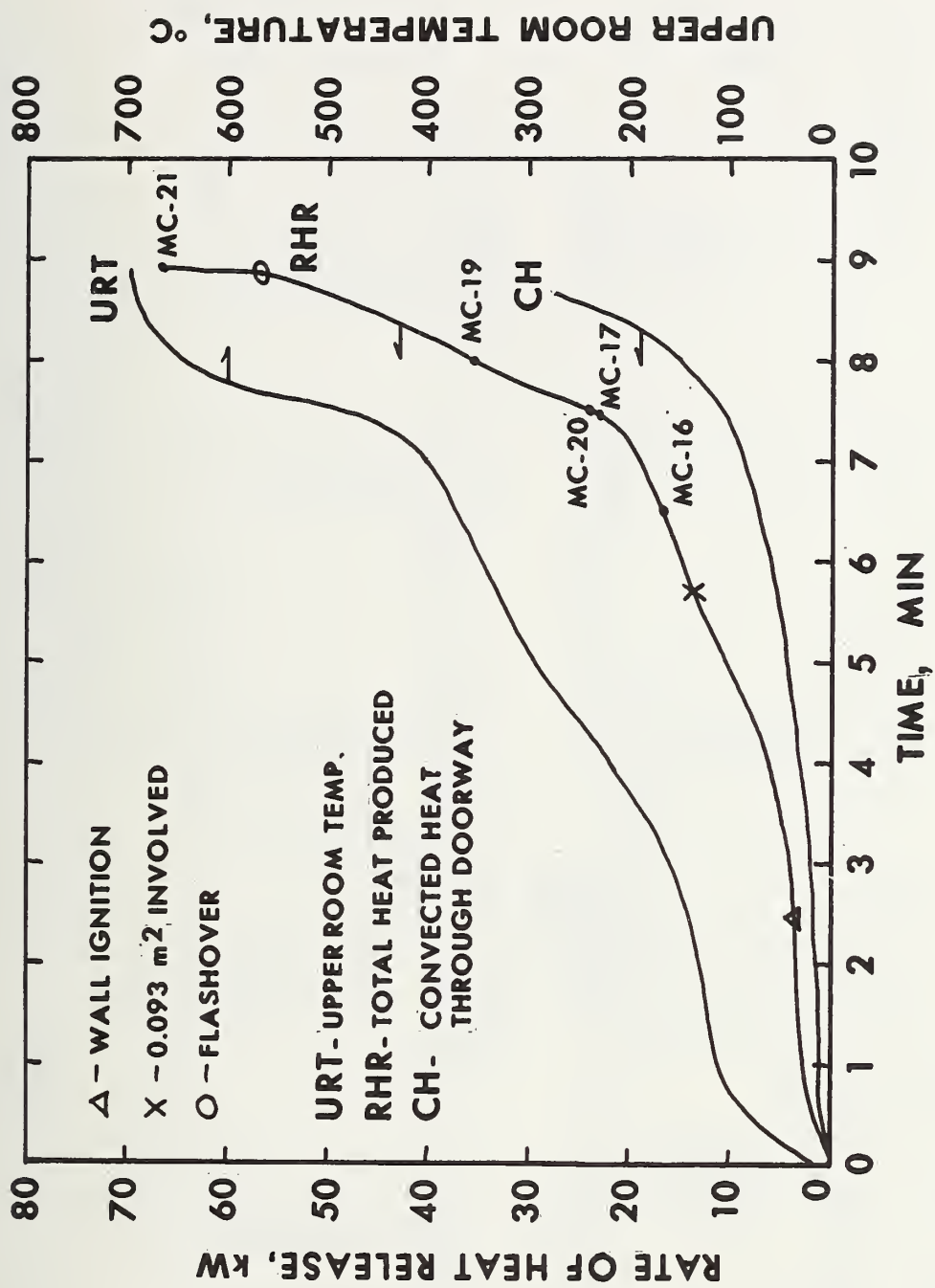
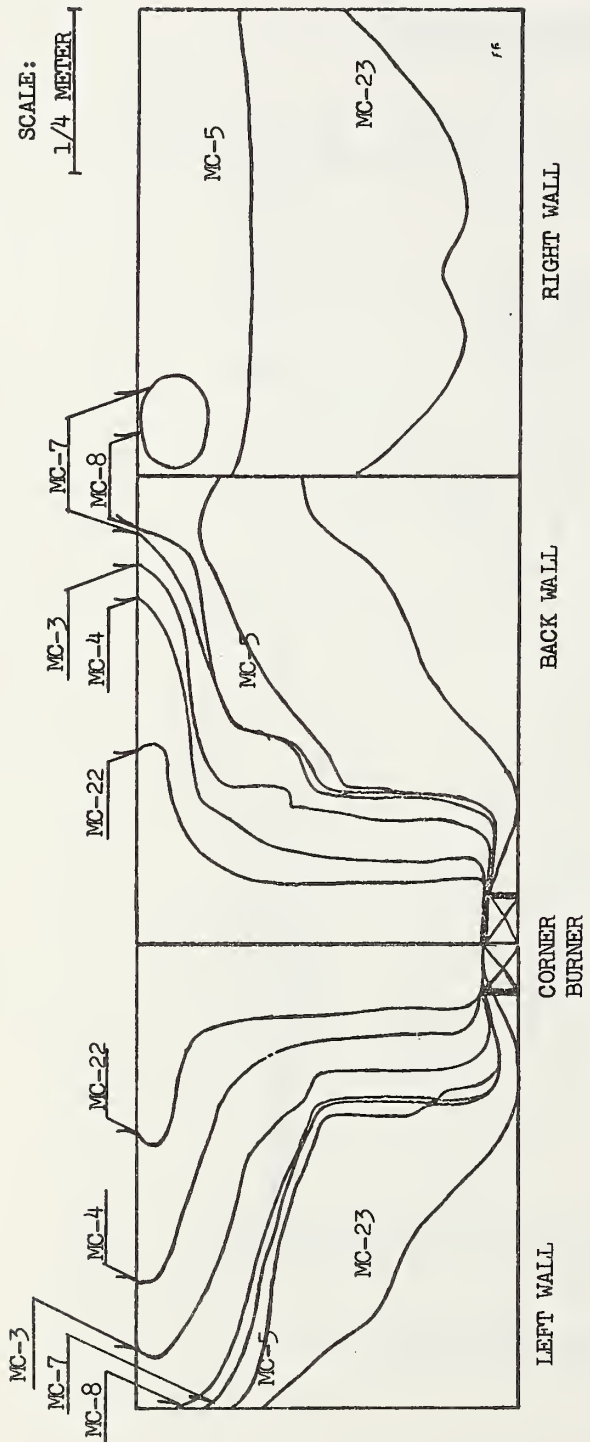
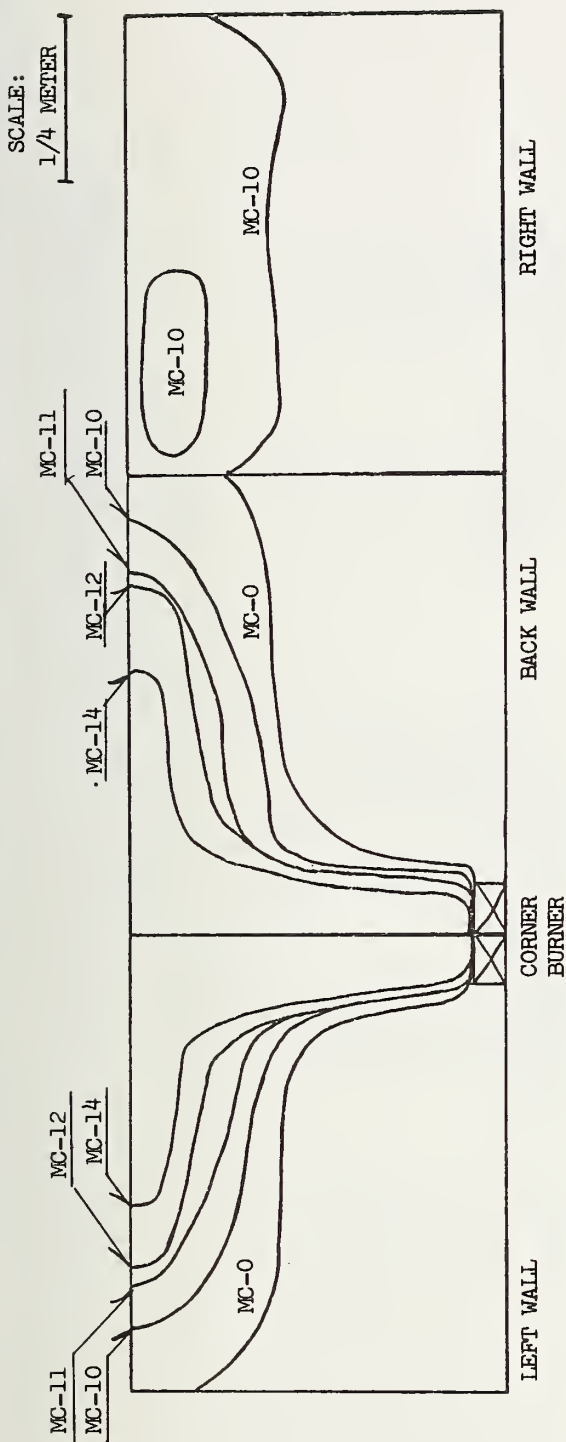


Figure 14. Model compartment results -- 2-ply 6-mm hardboard



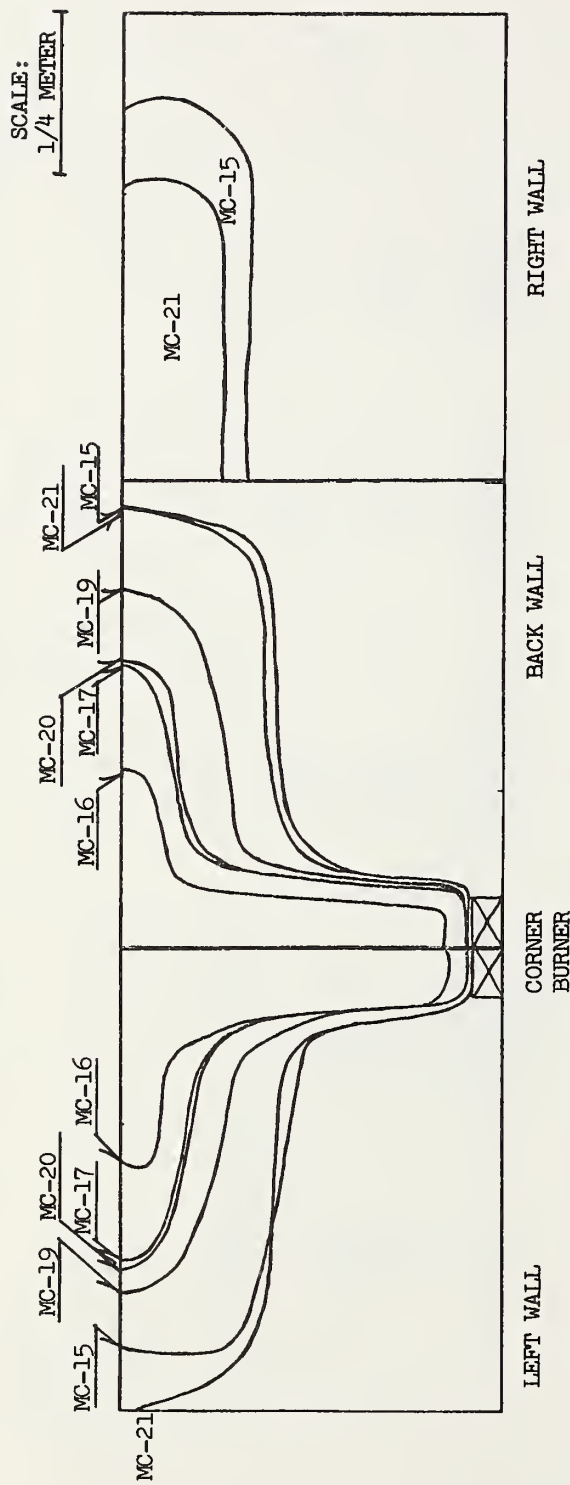
TEST	CORRECTED TERM. TIME		UPPER ROOM AIR TEMP., °C	INVOLVED, m <sup>2</sup>	AREA, m <sup>2</sup>	FIRE/AREA W/cm <sup>2</sup>
	MIN.	SEC				
MC-22	1:21		308	0.15	5.9	
MC-4	2:10		380	0.24	6.2	
MC-3	2:54		440	0.34	6.3	
MC-8	3:12		498	0.43	5.6	
MC-7	3:12		495	0.45	5.5	
MC-5	3:18		555	0.62	4.6	
MC-23	3:36	FO	782	1.06	6.9	
MC-6 (0% RH)	2:24	FO			1.34	
	2:33			796		6.9

Figure 15. Area of burning wall involved at various times to flashover, quarter-scale model compartment -- 12-mm low density wood fiberboard



TEST	CORRECTED TERM. MIN:SEC	UPPER ROOM AIR TEMP. °C	AREA INVOLVED. m <sup>2</sup>	RHR/AREA W/cm <sup>2</sup>
MC-14	5:24	380	0.16	9.4
MC-12	7:10	460	0.22	8.0
MC-11	7:45	565	0.25	10.6
MC-10	8:09	680	0.34	9.8
MC-0	8:45 FO 8:51	730	0.61	8.9
MC-13 (0% RH)	5:53 FO 5:59 TERM.	710	0.68	9.1

Figure 16. Area of burning wall involved at various times to flashover, quarter-scale model compartment -- 16-mm particleboard



TEST	CORRECTED TERM. TIME MIN:SEC	UPPER ROOM AIR TEMP., °C	AREA INVOLVED, m <sup>2</sup>	RHR/AREA W/cm <sup>2</sup>
			BACK WALL	
MC-16	6:30	376	0.13	11.1
MC-17	7:27	490	0.19	11.8
MC-20	7:30	500	0.19	12.2
MC-19	8:00	660	0.25	13.7
MC-21	8:54	710	0.48	14.0
MC-15	8:58 FO	720	0.51	15.9
MC-18 (0% RH)	6:05 FO 6:12	737	0.65	13.7

Figure 17. Area of burning wall involved at various times to flashover, quarter-scale model compartment -- 2 ply 6-mm hardboard

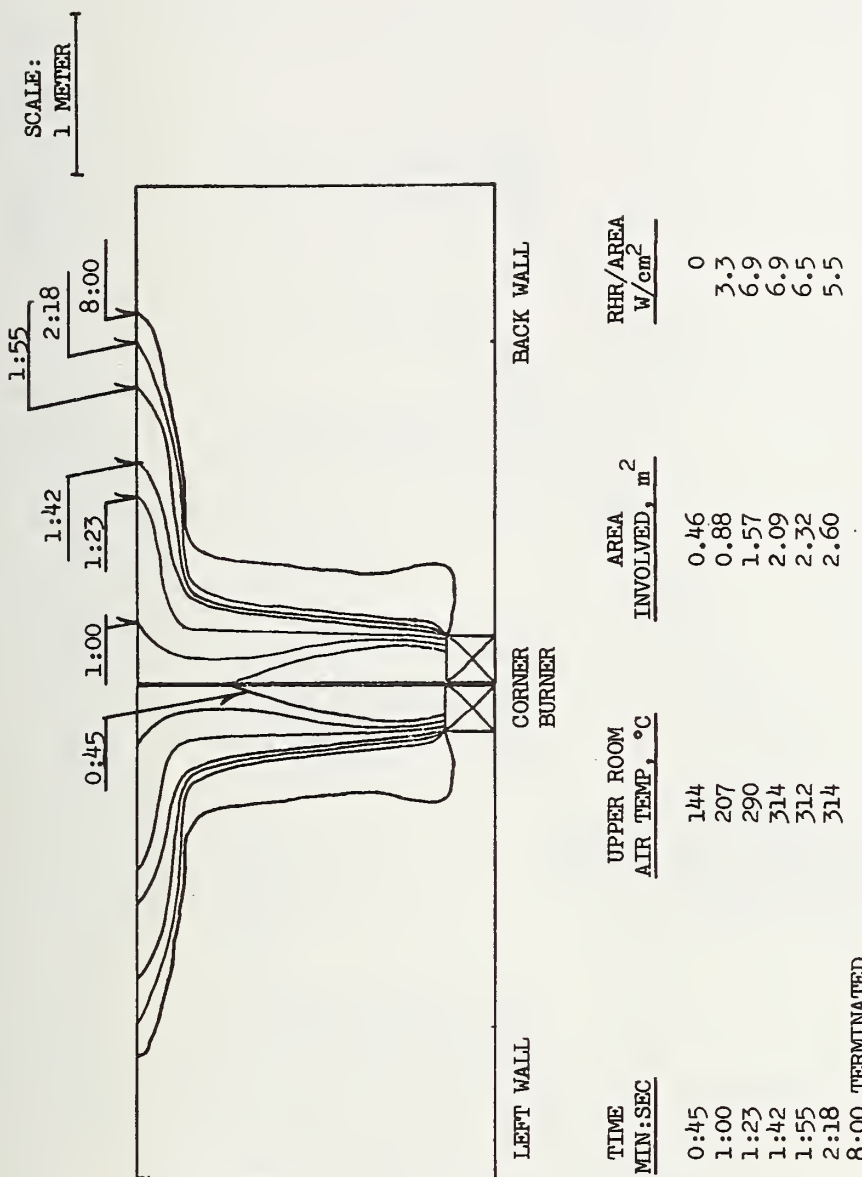


Figure 18. Area of burning wall involved at various times, full-scale room burn -- 12-mm low density wood fiberboard

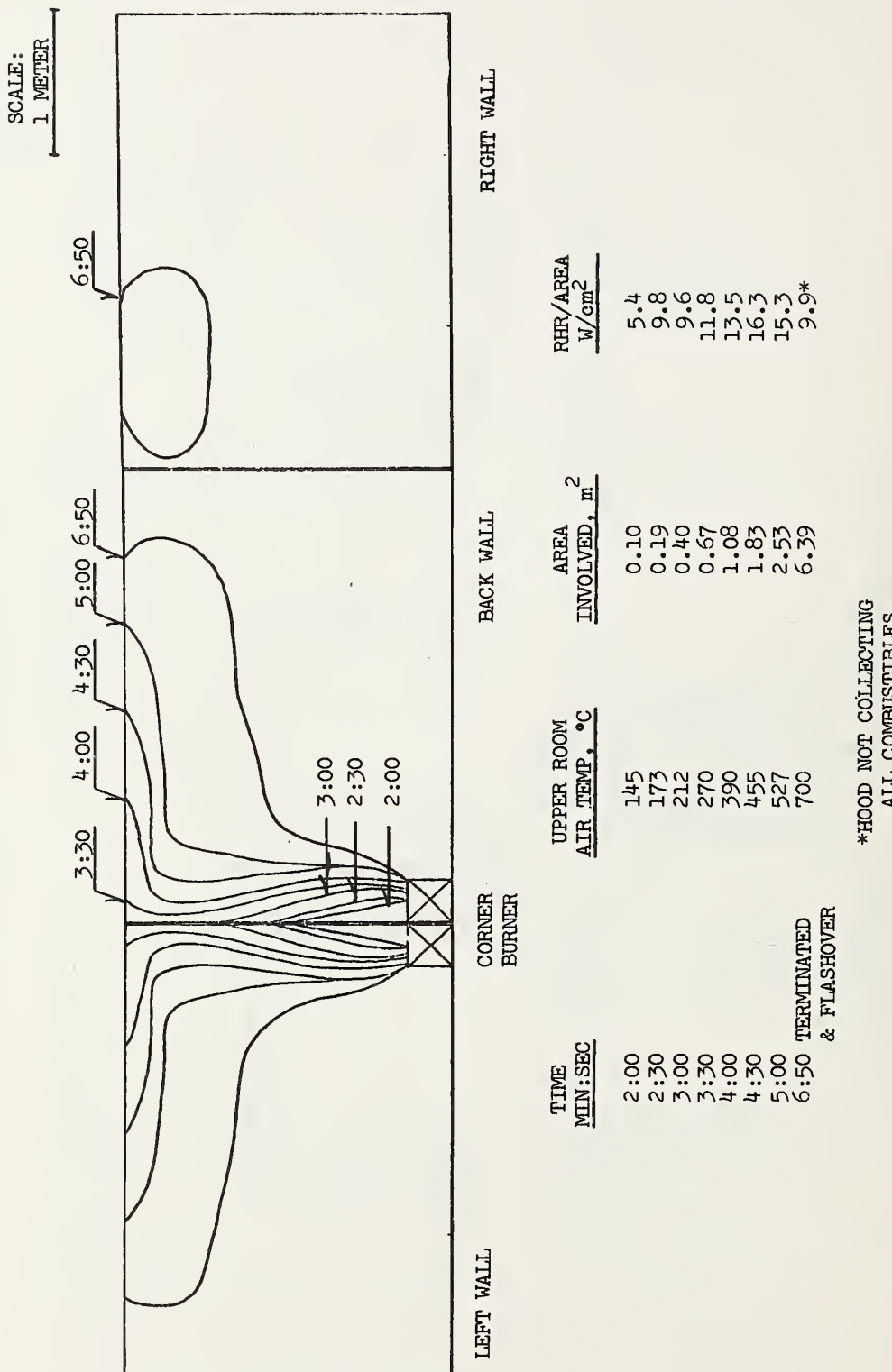


Figure 19. Area of burning wall involved at various times to flashover, full-scale room burn -- 2-ply 6-mm hardboard

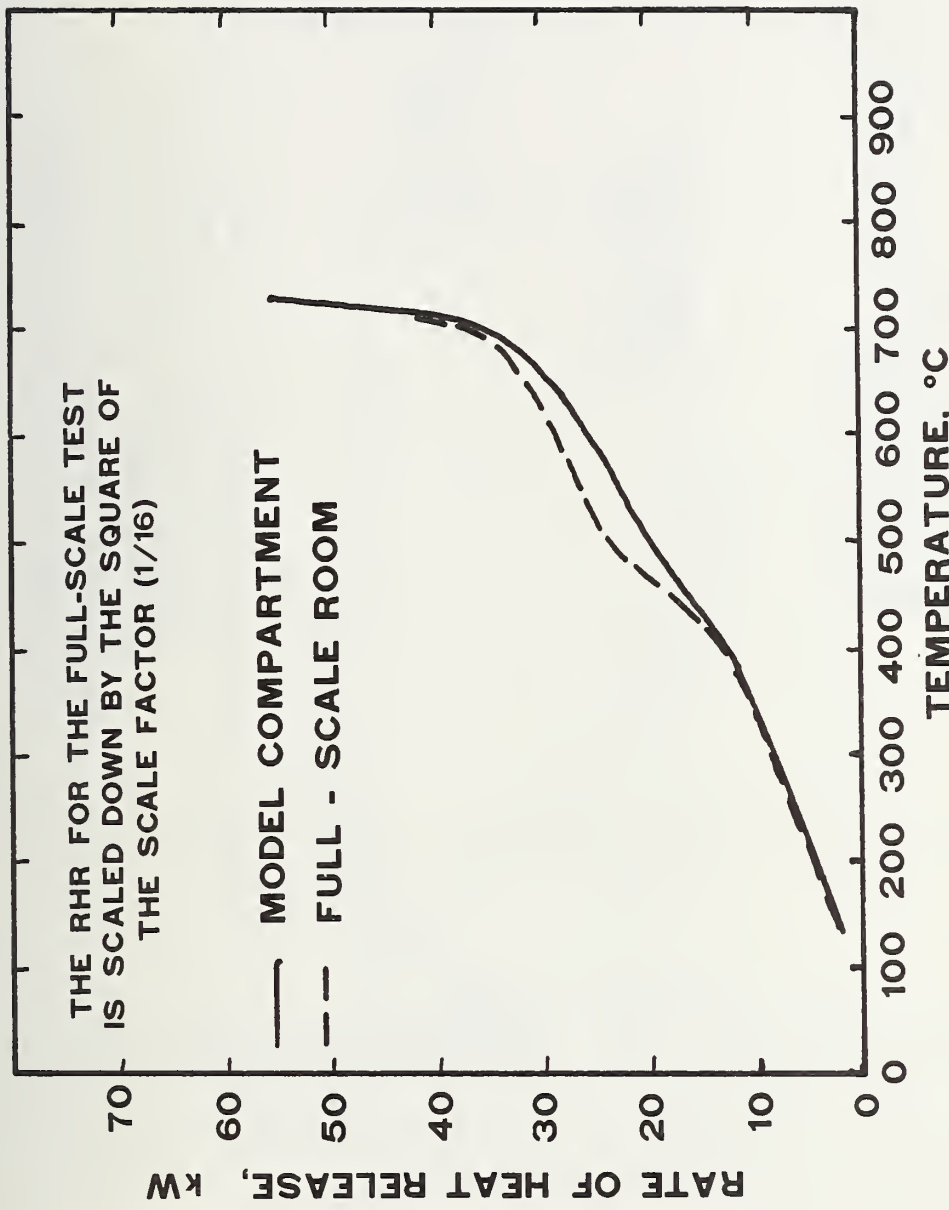


Figure 20. Upper room-air temperature in center of room for full- and quarter-scale enclosures lined with hardboard at 0% RH as a function of rate of heat release as determined by oxygen consumption

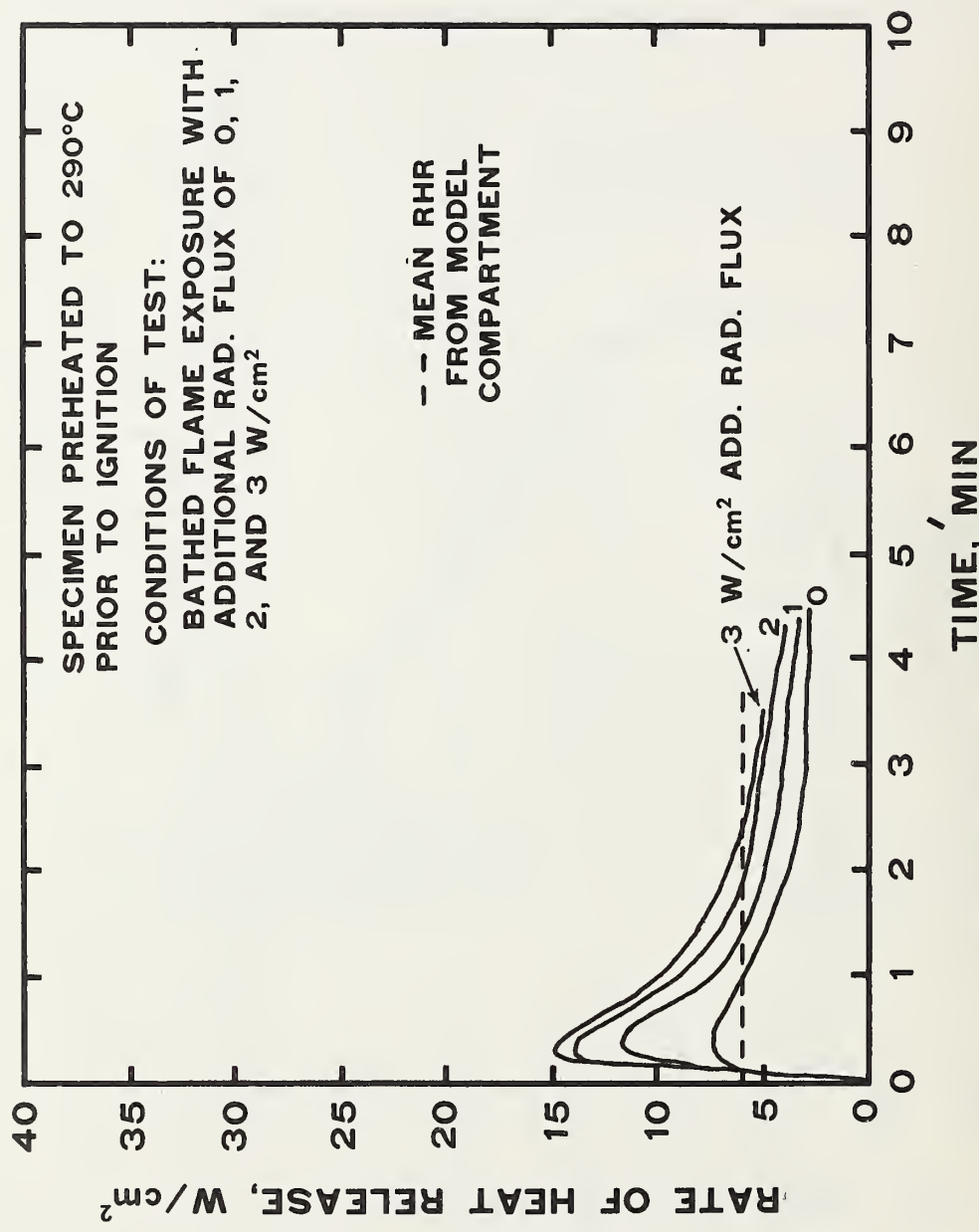


Figure 21. Rate of heat release -- low density wood fiberboard bench test results

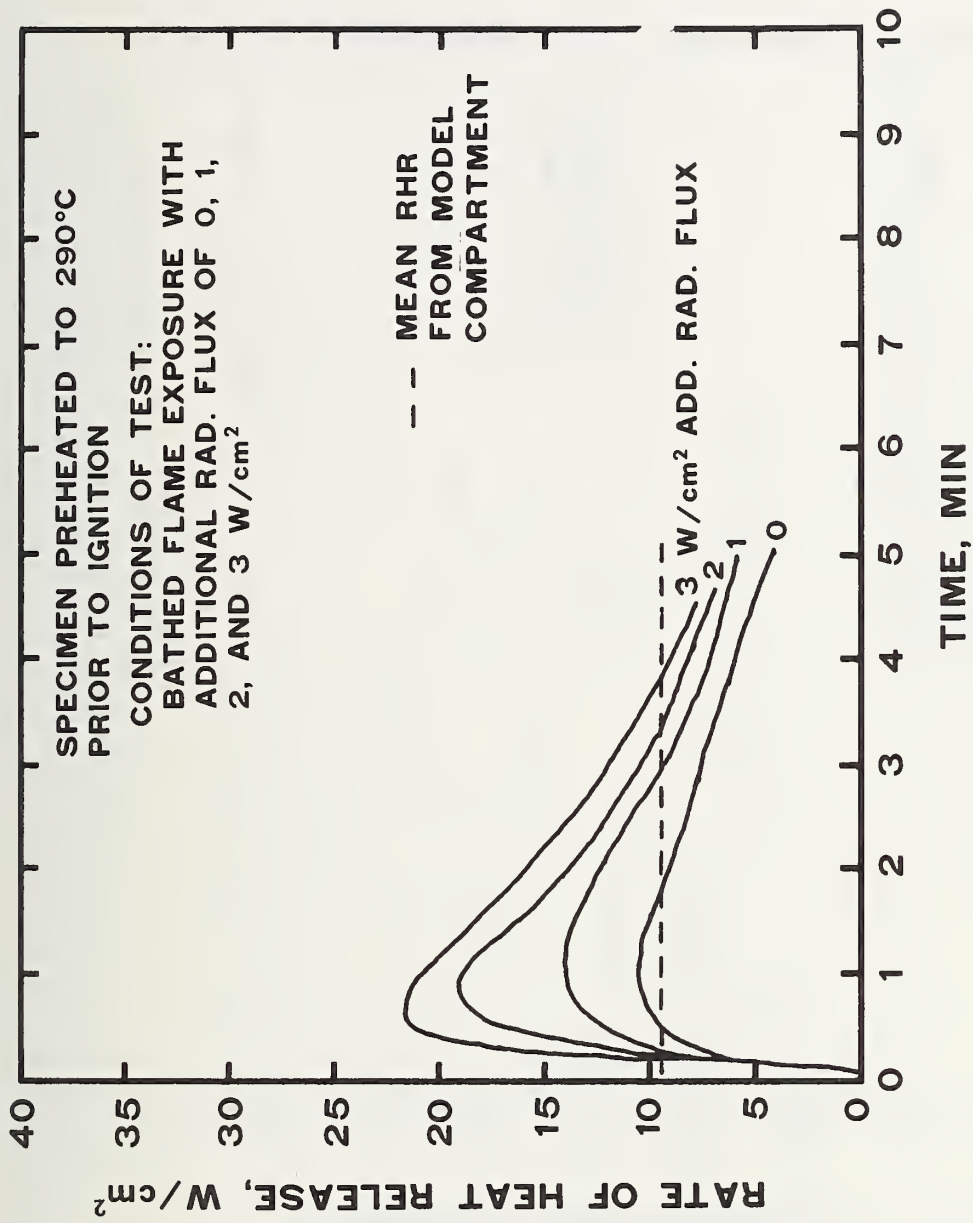


Figure 22. Rate of heat release -- particleboard bench test results

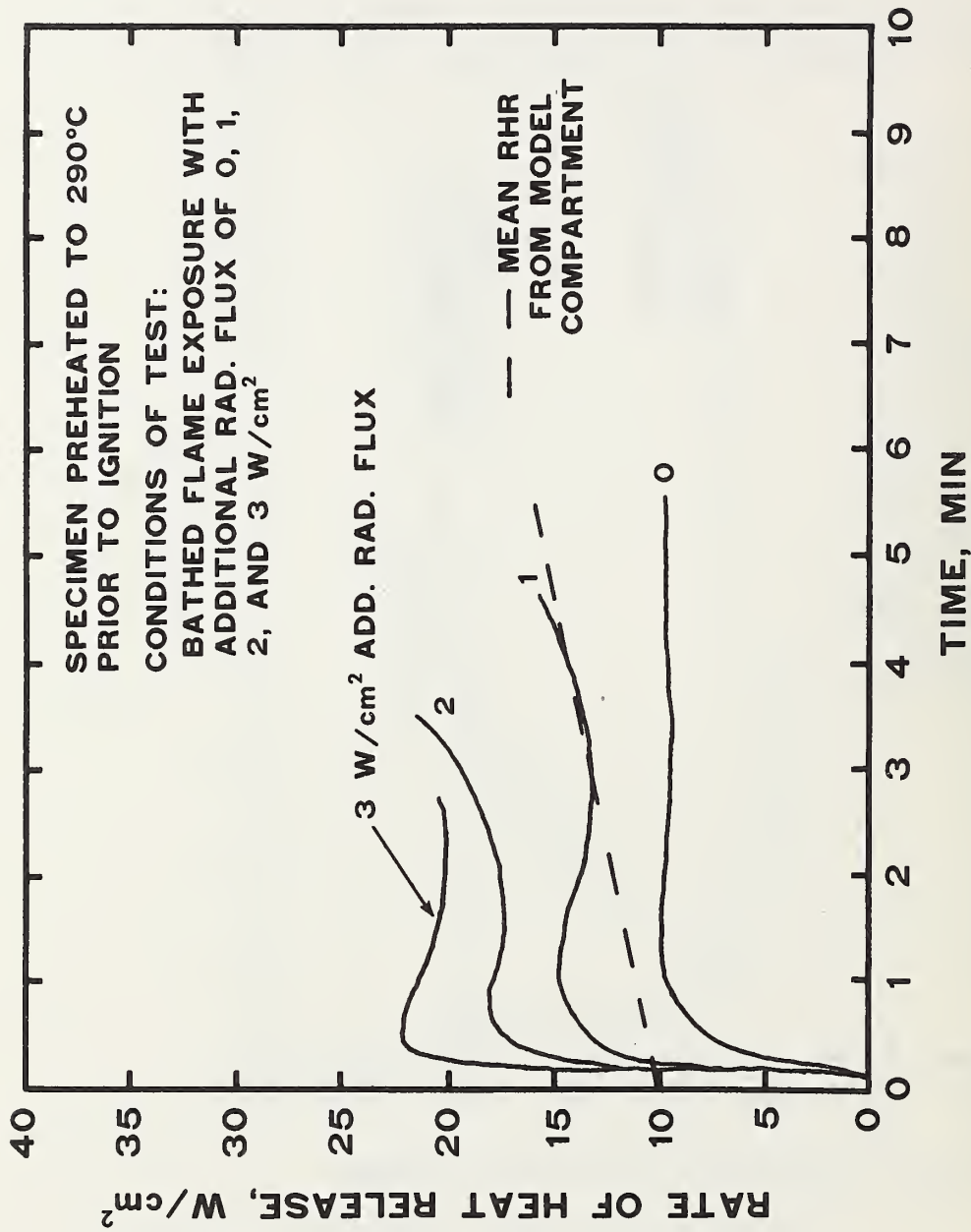


Figure 23. Rate of heat release -- hardboard bench test results

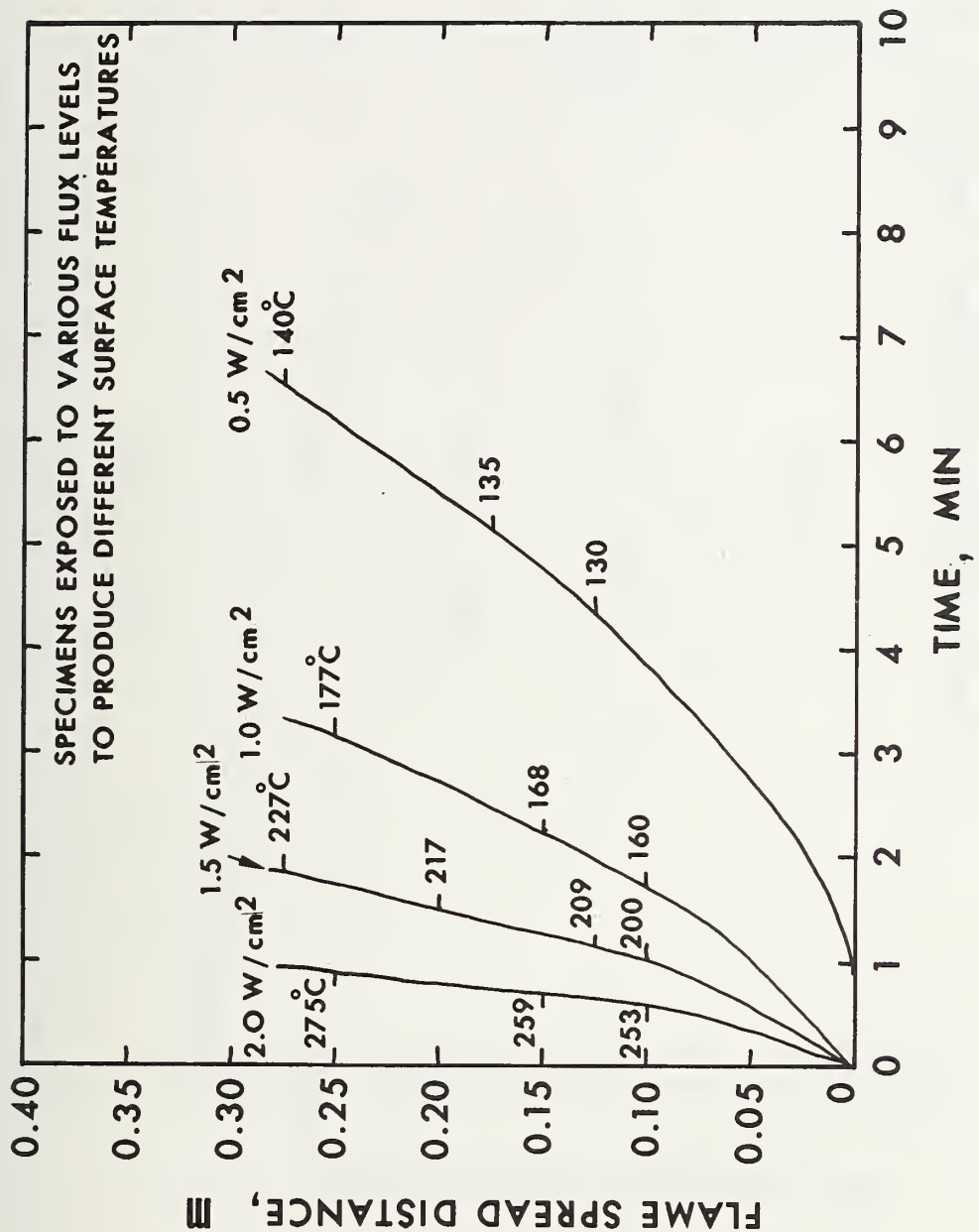


Figure 24. Flame spread distance vs time -- low density fiberboard

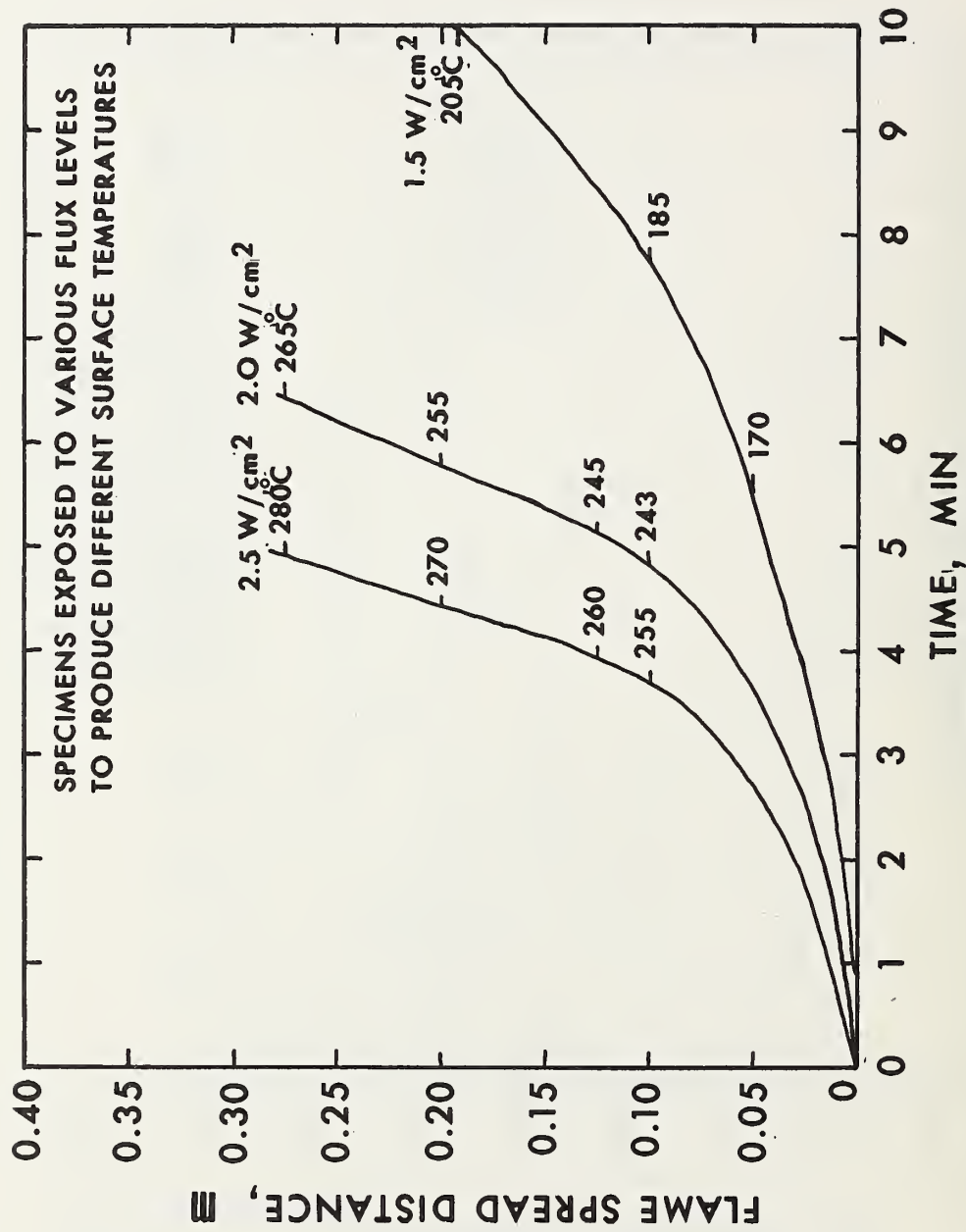


Figure 25. Flame spread distance vs time -- hardboard

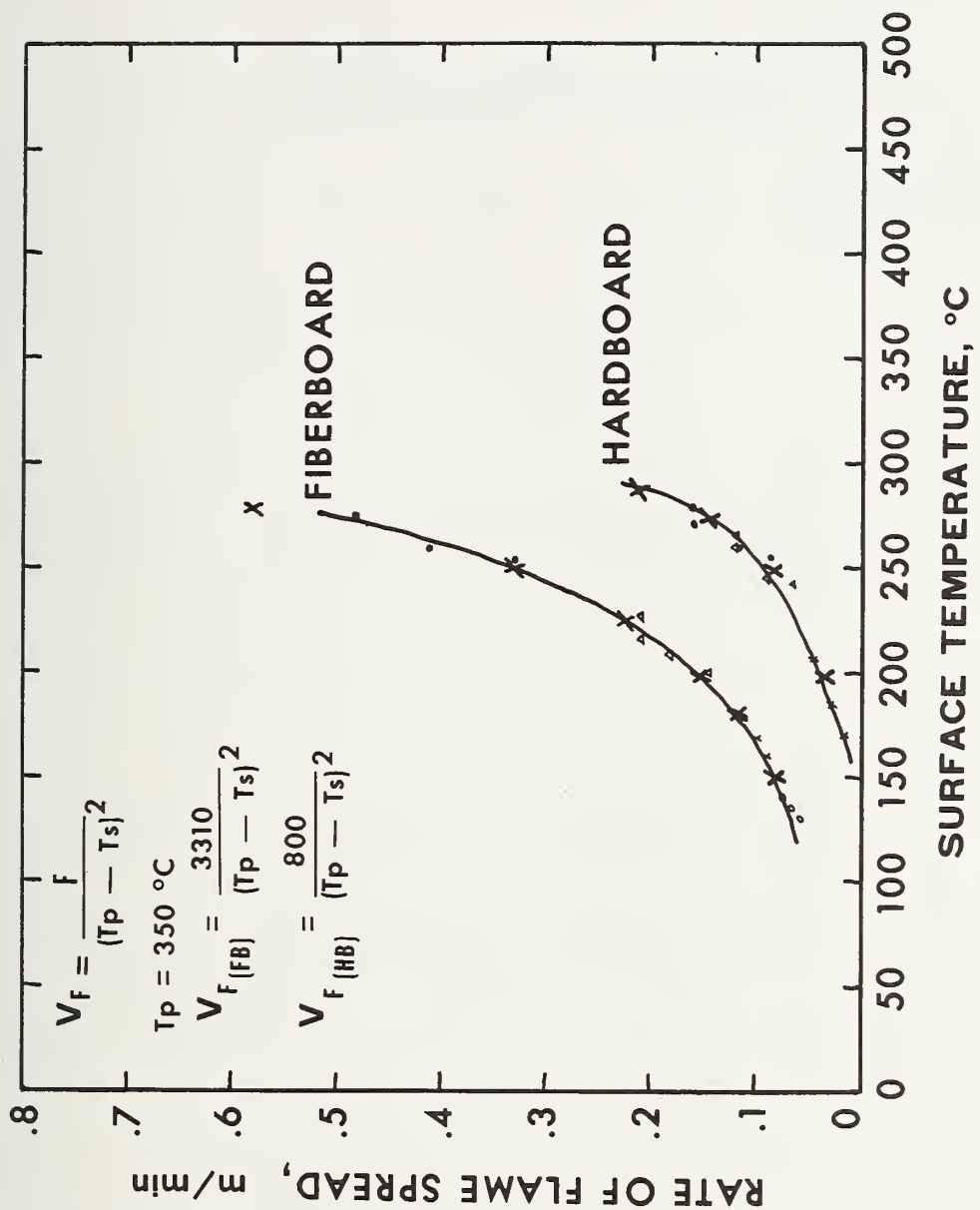


Figure 26. Rate of flame spread as a function of surface temperature

Table 1. Heat produced per volume of oxygen consumed for some common materials

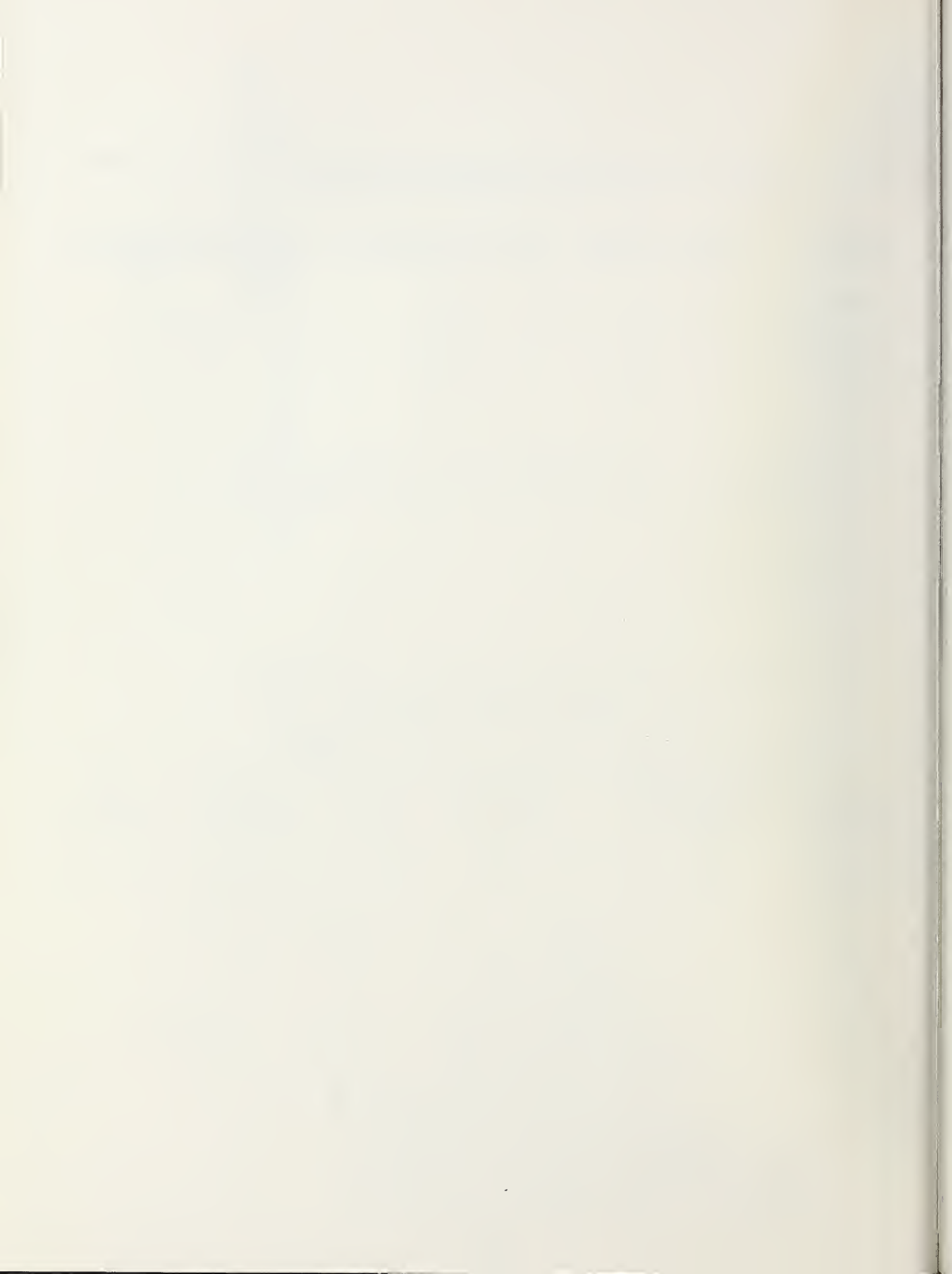
Materials	Heat of combustion Net MJ/kg	Oxygen requirement at 25°C (298 K) Net m <sup>3</sup> /kg	Heat produced per volume of oxygen consumed at 25°C (298 K)	
			Heat produced per volume of oxygen consumed at 25°C (298 K) Net MJ/m <sup>3</sup>	
Polyethylene	43.4	2.63	16.5	
Polypropylene	43.3	2.63	16.5	
Polystyrene	39.7	2.36	16.9	
Poly (Vinyl Chloride)	16.9	1.08	15.7	
6 Poly (Methyl Methacrylate)	25.2	1.47	17.1	
Phenol-Formaldehyde (1:1)	26.7	1.86	14.3	
Urea-Formaldehyde (1:2)	16.8	1.02	16.4	
Melamine-Formaldehyde (1:3)	18.4	1.14	16.3	
Polyurethane, Ester Based	22.4	1.32	17.0	
Unsaturated Polyesters	28.4	1.58	18.0	
Butadiene/Styrene (25.5%)	41.9	2.46	17.0	
Copolymer (GRS) Rubber	15.2	0.91	16.8	
Cellulose	32.8	2.05	16.0	
Carbon	120.6	6.14	19.6	
Hydrogen	50.2	3.01	16.4	
Methane				

Table 2. Comparison of effective net heats of combustion with actual gross and net heat of combustion (MJ/kg)

<u>Material</u>	<u>Bench RHR test</u>	<u>Model compartment</u>	<u>Oxygen bomb calorimeter</u>	
			<u>Gross</u>	<u>Net</u>
Fiberboard	13.5	12.5	18.8	17.2
Particleboard	12.5	10.0	19.4	17.7
Hardboard	12.5	11.0	19.7	18.0

Table 3. Data summary for prediction of flashover times in model compartment

<u>Material</u>	<u>Wall ignition time, (s)</u>	<u>Flashover time, (s)</u>	<u><math>\bar{q}</math></u> <u>kW/m<sup>2</sup></u>	<u>F</u> <u>K<sup>2</sup>·m/s</u>	<u>C<sub>4</sub></u> <u>K<sup>2</sup>·kW/m</u>
Fiberboard	27	216	60	55	$6.3 \times 10^5$
Hardboard	147	534	130	13.3	$6.7 \times 10^5$



## APPENDIX A

### Technical Data

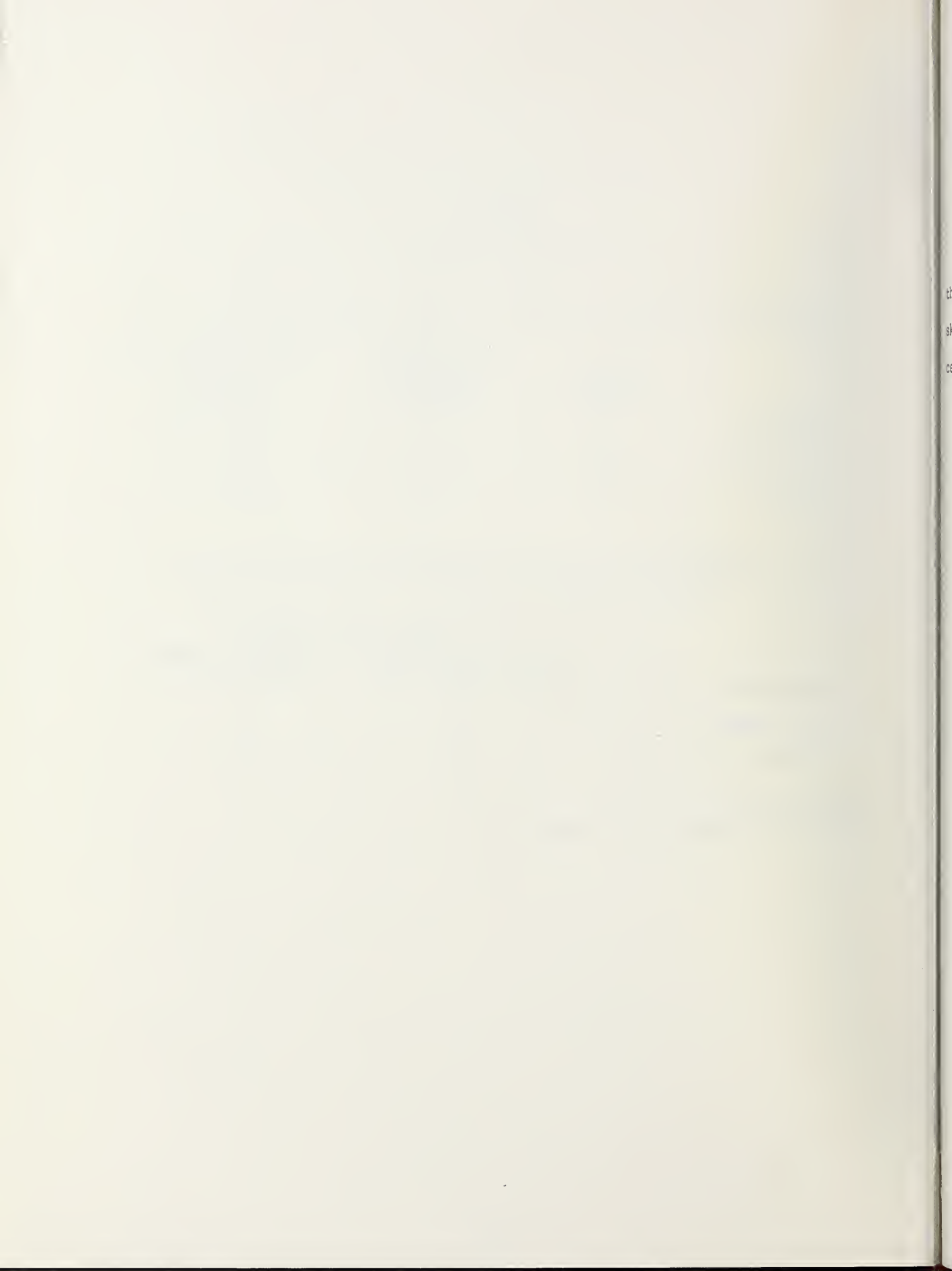
#### Thermophysical Properties of Materials Employed in This Experimental Study\*

	Density, kg/m <sup>3</sup>	Specific heat at 23°C kJ/(kg K)	Thermal conductivity at 23°C kW/(m K)
Fiberboard	307	1.43	55 x 10 <sup>-6</sup>
Particleboard	674	1.97	119 x 10 <sup>-6</sup>
Hardboard	900	1.49	126 x 10 <sup>-6</sup>

#### Ignition Times Obtained on the NBS Test for Ease of Ignition Compared With Time to Ignite Wall in Model Compartment

	Ignition time, seconds	
	Ease of ignition test	Model compartment
Fiberboard	20	27
Particleboard	96	108
Hardboard	103	147

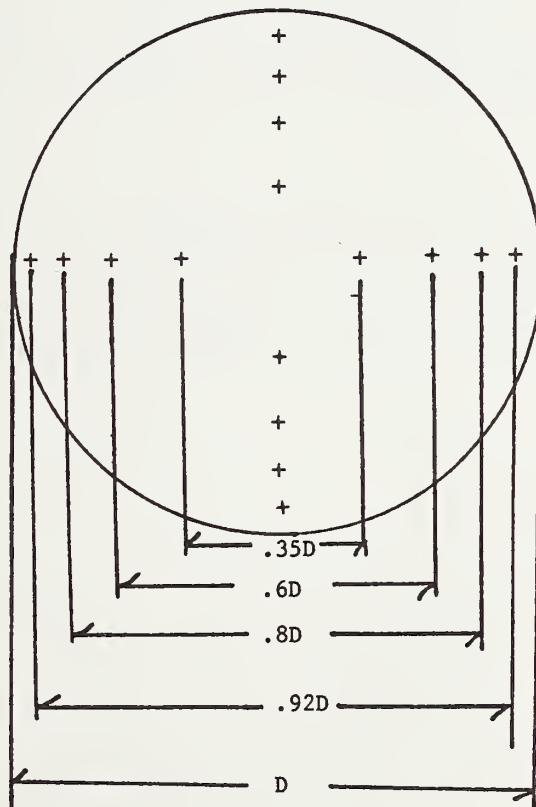
\*Measured at Armstrong Cork Company



## APPENDIX B

### Scanning Technique Used to Determine Mean Velocity Across the Exhaust Pipe Cross Section

A traverse of the pipe was made with the pitot-static tube, averaging the readings taken at positions marked "+" in the pipe according to the sketch. The factor,  $C_v$ , was obtained by dividing the average velocity by the center velocity over a range of flow rates.





## Crib Tests

An adjunct to this study included the burning of two cribs beneath the large room collection hood. This was done in order to demonstrate the applicability of this method of determining rate of heat release and effective heat of combustion from other large fires. The cribs each weighing 3.4 kg were constructed of polyurethane ( $320 \text{ kg/m}^3$ ) and sugar pine. Placement of the cribs on a load cell during burning permitted calculations for the rate of weight loss to determine effective heats of combustion. The rate of heat release as a function of time (RHR) was determined by oxygen consumption and is plotted in figure 27. The broken lines labeled A, A<sup>1</sup>, B, B<sup>1</sup>, etc. are plotted at the mean RHR associated with the computed rate of weight loss (RWL) over the same period.

The heat of combustion (HOC) was determined during each of these time intervals by dividing the RHR by the RWL. The increase in the HOC at latter times during intervals D and D<sup>1</sup> probably reflects the combustion of the char.

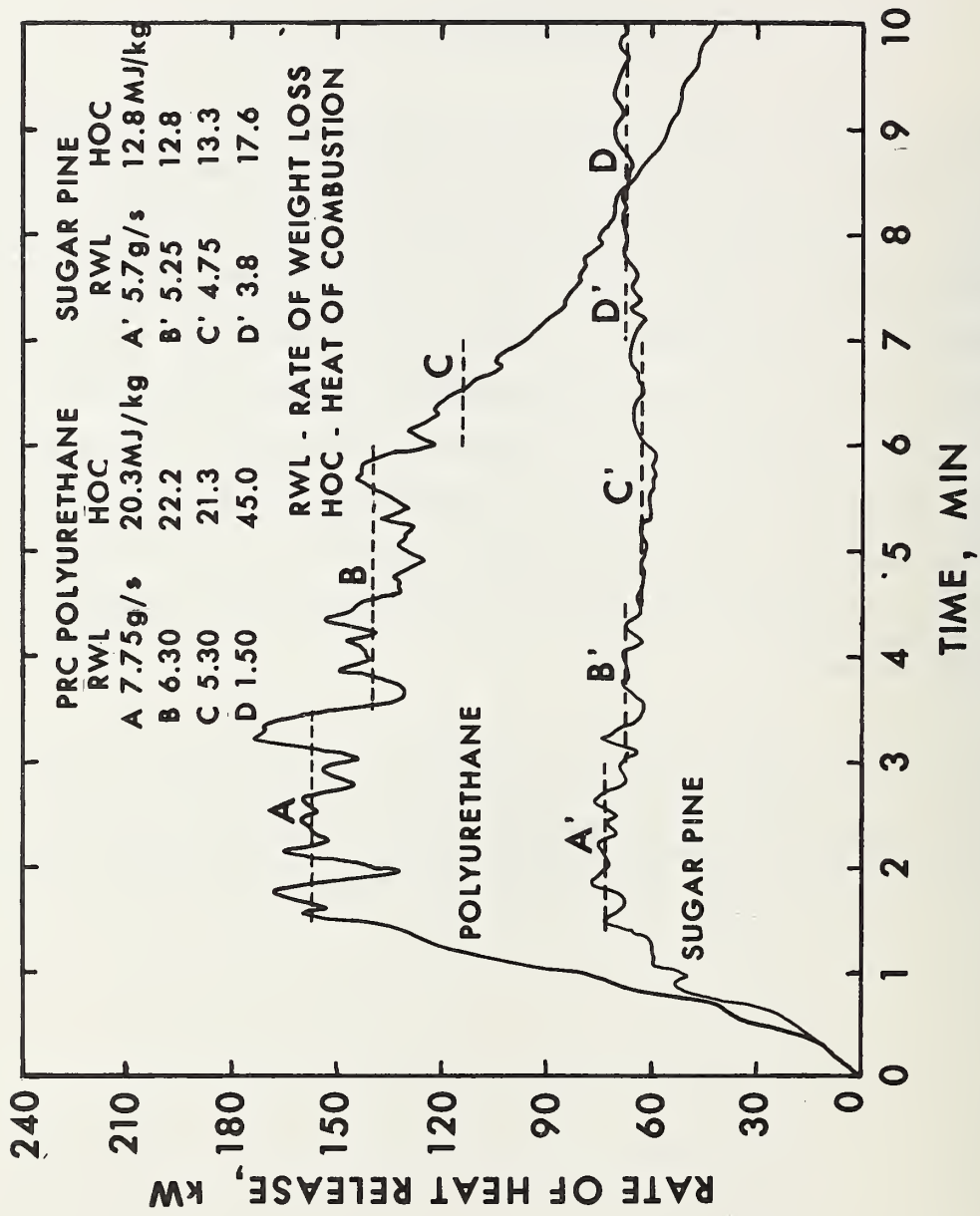


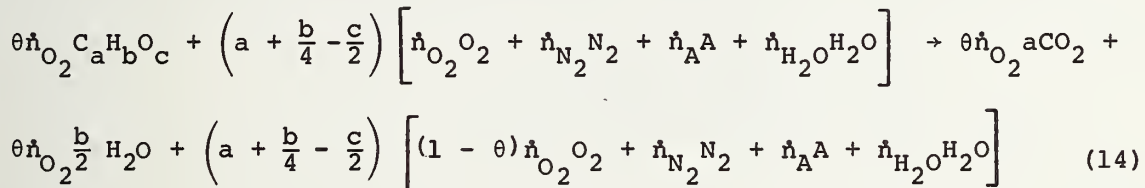
Figure 1C. Rate of heat release from 3.4 kg cribs of polyurethane and sugar pine under large hood

## APPENDIX D

### Errors in Calculation of the Rate of Heat Release

In section 2.1 it was assumed that (1) the molar flow rate of the combustion gases in the exhaust duct was equal to the molar flow rate of the air into the system, (2) the oxygen concentration in the analyzer was equal to that in the exhaust duct, (3) the ambient density of the stack gases was equal to that of air, (4) the concentration of CO in the exhaust gases was negligible, and (5) the incoming air was dry.

The errors due to the assumptions in section 2.1 will be examined for fuels of the form  $C_aH_bO_c$  which undergo the following complete reaction in air to  $CO_2$  and  $H_2O$ :



where  $\dot{n}_{O_2}$ ,  $\dot{n}_{N_2}$ ,  $\dot{n}_A$ , and  $\dot{n}_{H_2O}$  are the molar flow rates of oxygen, nitrogen, argon, and water vapor into the system. The oxygen depletion,  $\theta$ , is defined as the fraction of the incoming oxygen molecules that are removed by combustion.

Equation 2 can be more accurately written

$$\dot{Q} = 1.67 \times 10^4 x_o \dot{V}_a \theta = 1.67 \times 10^4 x_o \dot{V}_s \left( \frac{\dot{V}_a}{\dot{V}_s} \right) \theta \quad (15)$$

Equation 14 can be used to determine  $\frac{\dot{V}_a}{\dot{V}_s}$  and  $\theta$ .

The ratio of the molar flow rate of the gases leaving the system,  $\dot{n}_s$ , to the molar flow rate of the air entering the system  $\dot{n}_a$  is found from equation 14 to be

$$\frac{\dot{n}_s}{\dot{n}_a} = \frac{\dot{V}_s}{\dot{V}_a} = 1 + \frac{x_o \theta \left( \frac{b}{4} + \frac{c}{2} \right)}{a + \frac{b}{4} - \frac{c}{2}} \quad (16)$$

where  $x_o = \frac{\dot{n}_{O_2}}{\dot{n}_{O_2} + \dot{n}_{N_2} + \dot{n}_A + \dot{n}_{H_2O}}$  is the oxygen concentration of the ambient air and  $\dot{V}_s$  and  $\dot{V}_a$  are the volume flow rates of the gas in the exhaust duct and of the air entering the system respectively. These volume flow rates are referred to standard conditions of temperature and pressure.

The oxygen concentration  $x_c$  in the analyzer for the case where the water is trapped but  $CO_2$  is allowed to pass is also found from equation 14,

$$x_c = \frac{\left( a + \frac{b}{4} - \frac{c}{2} \right) (1 - \theta) x_o}{\left( 1 - x_H \right) \left( a + \frac{b}{4} - \frac{c}{2} \right) - \theta \left( \frac{b}{4} - \frac{c}{2} \right) x_o} \quad (17)$$

where  $x_H = \frac{\dot{n}_{H_2O}}{\dot{n}_{O_2} + \dot{n}_{N_2} + \dot{n}_A + \dot{n}_{H_2O}}$  is the volume fraction of water vapor in the ambient air.

Equation 17 can be solved for  $\theta$

$$\theta = \left[ \frac{\left( \frac{x_o}{1 - x_H} \right) - x_c}{\left( \frac{x_o}{1 - x_H} \right)} \right] \left[ 1 - \frac{\frac{b}{4} - \frac{c}{2} - x_c}{a + \frac{b}{4} - \frac{c}{2}} \right]^{-1} \quad (18)$$

Prior to the test  $\theta = 0$  and  $x_c = x_c^o = \frac{x_o}{1 - x_H}$  because of the trapping of the moisture in the ambient air. Hence

$$\theta = \left( \frac{x_c^o - x_c}{x_c^o} \right) \left( 1 - \left( \frac{b}{4} - \frac{c}{2} \right) x_c / \left( a + \frac{b}{4} - \frac{c}{2} \right) \right)^{-1} \quad (19)$$

Combining equations 15, 16, and 19

$$\dot{Q} = \frac{1.67 \times 10^4 x_o v_s (E_o - E)/E_o}{\left[1 + \theta x_o \left(\frac{b}{4} + \frac{c}{2}\right) / \left(a + \frac{b}{4} - \frac{c}{2}\right)\right] \left[1 - \left(\frac{b}{4} - \frac{c}{2}\right) x_c / \left(a + \frac{b}{4} - \frac{c}{2}\right)\right]} \quad (20)$$

where  $\frac{E_o - E}{E_o} = \frac{x_c^o - x_c}{x_c^o}$  is the fractional change in the voltage output of the analyzer assuming it is linear.

From equation 20 it can be seen that the only effect of the ambient humidity on the calculations is to reduce the value of  $x_o$  which is given by the relation

$$x_o = 0.2095 / (1 + x_H)^{-1} \quad (21)$$

where 0.2095 is the normal concentration of oxygen in dry air at sea level. However, if  $x_o$  is to be determined by the oxygen analyzer it must be done without the water being trapped. The volume fraction of water,  $x_H$ , is given by

$$x_H = 0.0224 (D/18) \frac{R}{100} \quad (22)$$

where D is the density of saturated water vapor in air in  $\text{g/m}^3$ . It is given as a function of temperature in the Handbook of Chemistry and Physics [8]. R is the relative humidity (RH) in percent. If  $x_o$  is taken to 0.208, its value for 20°C and 40% RH, its variation under normal conditions is less than 1%.

The factors in the denominator of equation 20 account for the difference in molar flow rates of the combustion gases in the stack and the incoming air and the difference between the oxygen concentration in the analyzer and in the stack. The numerator in equation 20 is essentially equation 2 which was used for the calculations during this project. The errors incurred by this procedure can be examined by writing equation 20 in terms of some common fuels.

For cellulose,  $C_6H_{10}O_5$

$$\dot{Q} = \frac{1.67 \times 10^4 x_o \dot{V}_s}{1 + 50 x_o/6} \left( \frac{E_o - E}{E_o} \right) \quad (23)$$

For methane,  $CH_4$

$$\dot{Q} = \frac{1.67 \times 10^4 x_o \dot{V}_s}{(1 + \theta x_o/2)(1 - x_c/2)} \left( \frac{E_o - E}{E_o} \right) \quad (24)$$

For  $-CH_2-$  polymers

$$\dot{Q} = \frac{1.67 \times 10^4 x_o \dot{V}_s}{(1 + \theta x_o/3)(1 - x_c/3)} \left( \frac{E_o - E}{E_o} \right) \quad (25)$$

For cellulose the error is negligible at low oxygen depletions but reaches 9% at a depletion of 0.5. For methane even at  $\theta = 0$  there is a 10.5% error which reduces to a 0.3% error at  $\theta = 0.5$ . For  $-CH_2-$  polymers the error at  $\theta = 0$  is 7% and less than 0.2% at  $\theta = 0.5$ .

Other sources of error considered to be small were gases generated in the fire and not converted to  $CO_2$  and  $H_2O$ . Also neglected was the consideration of CO present in the stack and in the cell. Since the heat release per volume of  $O_2$  consumed is substantially greater for CO than for other fuels the presence of CO leads to another error in heat release rate calculation. The heat of combustion of CO is  $11.76 \text{ MJ/m}^3$  at  $20^\circ\text{C}$  [15]. Then the heat released per volume of  $O_2$  consumed is  $23.2 \text{ MJ/m}^3$  at  $25^\circ\text{C}$ . The direct combustion of carbon to  $CO_2$  yields  $16.7 \text{ MJ/m}^3$  at  $25^\circ\text{C}$ . Then the heat produced per volume of  $O_2$  consumed in oxidizing the fuel to CO is  $8.8 \text{ MJ/m}^3$  (i.e.,  $8.8 = 2(16.0) - 23.2$ ). After flashover in a room fire CO levels can reach as high as 11% in the exhaust gases at the doorway when the oxygen concentration has gone nearly to zero [16]. In this extreme case, approximately 25% of the oxygen consumed has gone into CO production. Then the total rate of heat release will be 13% less than that calculated based on  $16.7 \text{ MJ/m}^3$  for all of the fuel being completely oxidized. Again a correction can be made if the CO

concentration is monitored in the stack gases. Also due to burning outside of the doorway much of the CO will be converted to CO<sub>2</sub> prior to the gas sampling point in the exhaust stack.

In calculating the volume flow rate in the stack, it was assumed that the ambient density of the stack gases was that of air. In order to account for the effect of the ambient density of the stack gases,  $\rho_s$ , on the calculation of the volume flow rate using the pitot-static tube it is necessary to replace  $\rho_o$  by  $\rho_s$  in equation 3 and rewrite in the form,

$$\dot{v}_s = C_v A \left( \frac{\rho_o}{\rho_s} \right)^{1/2} \left( \frac{2}{\rho_o} \frac{P_o}{P} \frac{T_o}{T} \right)^{1/2} (\Delta P)^{1/2} \quad (26)$$

Then  $\left( \frac{\rho_o}{\rho_s} \right)^{1/2}$  becomes the correction factor. Assuming dry air, the stack gas density in g/mole,  $\rho_s^*$ , deduced from equation 14 is given by

$$\rho_s^* = \frac{0.21\theta (44a + 9b) + a + \frac{b}{4} - \frac{c}{2} (29.0 - 6.72\theta)}{0.21\theta a + \frac{b}{2} + a + \frac{b}{4} - \frac{c}{2} (1 - 0.21\theta)} \quad (27)$$

For cellulose this becomes

$$\rho_s^* = \frac{174 + 34\theta}{6 + 1.05\theta} \quad (28)$$

For  $\theta = 0$        $\rho_s^* = \rho_o^* = 29.0$

For  $\theta = 1$        $\rho_s^* = 29.5$

For complete depletion of the oxygen the correction factor  $\left( \frac{\rho_o^*}{\rho_s^*} \right)^{1/2} = \left( \frac{\rho_o}{\rho_s} \right)^{1/2} = 0.991$  or a maximum error of 1% for cellulosic materials.

For methane

$$\rho_s^* = \frac{58 + 3.36\theta}{2 + 0.21\theta} \quad (29)$$

$$\left( \frac{\rho_o}{\rho_s} \right)^{1/2} = 1.022 \text{ for } \theta = 1$$

or a maximum error of 2%.

For  $-\text{CH}_2-$  polymers

$$\rho^* = \frac{43.5 + 2.94\theta}{1.5 + 0.105\theta} \quad (30)$$

$$\left( \frac{\rho_o}{\rho_s} \right)^{1/2} = 1.001 \text{ for } \theta = 1$$

or a maximum error of 0.1%.

Since the oxygen depletion factor,  $\theta$ , is normally much less than unity the effect of the chemical composition of the combustion gases on the ambient density of the stack gases can be neglected.

<p>U.S. DEPT. OF COMM. BIBLIOGRAPHIC DATA SHEET</p>				1. PUBLICATION OR REPORT NO. NBS Tech Note 1128	2. Gov't. Accession No.	3. Recipient's Accession No.
<p>4. TITLE AND SUBTITLE</p> <p>AN OXYGEN CONSUMPTION TECHNIQUE FOR DETERMINING THE CONTRIBUTION OF INTERIOR WALL FINISHES TO ROOM FIRES</p>				5. Publication Date July 1980	6. Performing Organization Code	
<p>7. AUTHOR(S) Darryl L. Sensenig</p>				8. Performing Organ. Report No.		
<p>9. PERFORMING ORGANIZATION NAME AND ADDRESS  NATIONAL BUREAU OF STANDARDS DEPARTMENT OF COMMERCE WASHINGTON, DC 20234</p>				10. Project/Task/Work Unit No.		
<p>12. SPONSORING ORGANIZATION NAME AND COMPLETE ADDRESS (Street, City, State, ZIP)  Sponsored in part by: Armstrong Cork Company Lancaster, Pennsylvania 17604</p>				13. Type of Report & Period Covered Final		
<p>15. SUPPLEMENTARY NOTES</p> <p><input type="checkbox"/> Document describes a computer program; SF-185, FIPS Software Summary, is attached.</p>				14. Sponsoring Agency Code		
<p>16. ABSTRACT (A 200-word or less factual summary of most significant information. If document includes a significant bibliography or literature survey, mention it here.)</p> <p>An oxygen consumption technique was developed for determining the total rate of heat production in a room fire. This was accomplished by measuring the volume flow rate and the oxygen concentration of the exhaust gases flowing through a collection hood. This method can be used with unknown combinations of burning materials including both interior finish and furnishings. By simultaneously measuring the rate of oxygen consumption and the rate of mass loss the effective heat of combustion of the wall linings were determined in a reduced-scale model room fire test. The average heat release rate per unit area of the wall linings was determined by recording the area of involvement during the test and dividing this area into the total rate of heat production at that time. The enthalpy of the exhaust gases passing out of the doorway was determined with the aid of an array of thermocouples located at the entrance to the exhaust duct. By subtracting the enthalpy flow through the doorway from the total rate of heat production in the room, the heat losses through the bounding surfaces were determined. Reduced-scale and full-scale room fire tests and a bench test for heat release rate using the oxygen consumption technique are discussed in this report. Lateral flame spread rates on vertical surfaces measured in the model room fire tests and in a laboratory bench test are also described.</p>						
<p>17. KEY WORDS (six to twelve entries; alphabetical order; capitalize only the first letter of the first key word unless a proper name; separated by semicolons)</p> <p>Fire tests; flame spread; flashover; heat release rate; ignition; interior finish; oxygen depletion; room fires.</p>						
<p>18. AVAILABILITY</p> <p><input checked="" type="checkbox"/> Unlimited</p> <p><input type="checkbox"/> For Official Distribution. Do Not Release to NTIS</p> <p><input checked="" type="checkbox"/> Order From Sup. of Doc., U.S. Government Printing Office, Washington, DC 20402</p> <p><input type="checkbox"/> Order From National Technical Information Service (NTIS), Springfield, VA. 22161</p>			<p>19. SECURITY CLASS (THIS REPORT)</p> <p>UNCLASSIFIED</p> <p>20. SECURITY CLASS (THIS PAGE)</p> <p>UNCLASSIFIED</p>		<p>21. NO. OF PRINTED PAGES</p> <p>87</p> <p>22. Price</p> <p>\$3.75</p>	



# NBS TECHNICAL PUBLICATIONS

## PERIODICALS

**JOURNAL OF RESEARCH**—The Journal of Research of the National Bureau of Standards reports NBS research and development in those disciplines of the physical and engineering sciences in which the Bureau is active. These include physics, chemistry, engineering, mathematics, and computer sciences. Papers cover a broad range of subjects, with major emphasis on measurement methodology and the basic technology underlying standardization. Also included from time to time are survey articles on topics closely related to the Bureau's technical and scientific programs. As a special service to subscribers each issue contains complete citations to all recent Bureau publications in both NBS and non-NBS media. Issued six times a year. Annual subscription: domestic \$13; foreign \$16.25. Single copy, \$3 domestic; \$3.75 foreign.

NOTE: The Journal was formerly published in two sections: Section A "Physics and Chemistry" and Section B "Mathematical Sciences."

**DIMENSIONS/NBS**—This monthly magazine is published to inform scientists, engineers, business and industry leaders, teachers, students, and consumers of the latest advances in science and technology, with primary emphasis on work at NBS. The magazine highlights and reviews such issues as energy research, fire protection, building technology, metric conversion, pollution abatement, health and safety, and consumer product performance. In addition, it reports the results of Bureau programs in measurement standards and techniques, properties of matter and materials, engineering standards and services, instrumentation, and automatic data processing. Annual subscription: domestic \$11; foreign \$13.75.

## NONPERIODICALS

**Monographs**—Major contributions to the technical literature on various subjects related to the Bureau's scientific and technical activities.

**Handbooks**—Recommended codes of engineering and industrial practice (including safety codes) developed in cooperation with interested industries, professional organizations, and regulatory bodies.

**Special Publications**—Include proceedings of conferences sponsored by NBS, NBS annual reports, and other special publications appropriate to this grouping such as wall charts, pocket cards, and bibliographies.

**Applied Mathematics Series**—Mathematical tables, manuals, and studies of special interest to physicists, engineers, chemists, biologists, mathematicians, computer programmers, and others engaged in scientific and technical work.

**National Standard Reference Data Series**—Provides quantitative data on the physical and chemical properties of materials, compiled from the world's literature and critically evaluated. Developed under a worldwide program coordinated by NBS under the authority of the National Standard Data Act (Public Law 90-396).

**NOTE:** The principal publication outlet for the foregoing data is the *Journal of Physical and Chemical Reference Data (JPCRD)* published quarterly for NBS by the American Chemical Society (ACS) and the American Institute of Physics (AIP). Subscriptions, reprints, and supplements available from ACS, 1155 Sixteenth St., NW, Washington, DC 20056.

**Building Science Series**—Disseminates technical information developed at the Bureau on building materials, components, systems, and whole structures. The series presents research results, test methods, and performance criteria related to the structural and environmental functions and the durability and safety characteristics of building elements and systems.

**Technical Notes**—Studies or reports which are complete in themselves but restrictive in their treatment of a subject. Analogous to monographs but not so comprehensive in scope or definitive in treatment of the subject area. Often serve as a vehicle for final reports of work performed at NBS under the sponsorship of other government agencies.

**Voluntary Product Standards**—Developed under procedures published by the Department of Commerce in Part 10, Title 15, of the Code of Federal Regulations. The standards establish nationally recognized requirements for products, and provide all concerned interests with a basis for common understanding of the characteristics of the products. NBS administers this program as a supplement to the activities of the private sector standardizing organizations.

**Consumer Information Series**—Practical information, based on NBS research and experience, covering areas of interest to the consumer. Easily understandable language and illustrations provide useful background knowledge for shopping in today's technological marketplace.

*Order the above NBS publications from: Superintendent of Documents, Government Printing Office, Washington, DC 20402.*

*Order the following NBS publications—FIPS and NBSIR's—from the National Technical Information Services, Springfield, VA 22161.*

**Federal Information Processing Standards Publications (FIPS PUB)**—Publications in this series collectively constitute the Federal Information Processing Standards Register. The Register serves as the official source of information in the Federal Government regarding standards issued by NBS pursuant to the Federal Property and Administrative Services Act of 1949 as amended, Public Law 89-306 (79 Stat. 1127), and as implemented by Executive Order 11717 (38 FR 12315, dated May 11, 1973) and Part 6 of Title 15 CFR (Code of Federal Regulations).

**NBS Interagency Reports (NBSIR)**—A special series of interim or final reports on work performed by NBS for outside sponsors (both government and non-government). In general, initial distribution is handled by the sponsor; public distribution is by the National Technical Information Services, Springfield, VA 22161, in paper copy or microfiche form.

## BIBLIOGRAPHIC SUBSCRIPTION SERVICES

The following current-awareness and literature-survey bibliographies are issued periodically by the Bureau:

**Cryogenic Data Center Current Awareness Service.** A literature survey issued biweekly. Annual subscription: domestic \$25; foreign \$30.

**Liquefied Natural Gas.** A literature survey issued quarterly. Annual subscription: \$20.

**Superconducting Devices and Materials.** A literature survey issued quarterly. Annual subscription: \$30. Please send subscription orders and remittances for the preceding bibliographic services to the National Bureau of Standards, Cryogenic Data Center (736) Boulder, CO 80303.

**U.S. DEPARTMENT OF COMMERCE**  
**National Bureau of Standards**  
Washington, D.C. 20234

—  
OFFICIAL BUSINESS

Penalty for Private Use, \$300

POSTAGE AND FEES PAID  
U.S. DEPARTMENT OF COMMERCE  
COM-215



SPECIAL FOURTH-CLASS RATE  
BOOK

---